Summer 2019

Satellites, Seagrass, and Blue Crabs: Understanding Inter-Annual Fluctuations and Linkages in the York River

Kristen Bachand
William & Mary - Virginia Institute of Marine Science, kebachand18@gmail.com

Satellites, Seagrass, and Blue Crabs: Understanding Inter-Annual Fluctuations and Linkages in the York River

---

A Thesis

Presented to

The Faculty of the School of Marine Science

The College of William & Mary

In Partial Fulfillment

of the Requirements for the Degree of

Master of Science

By

Kristen E. Bachand

August 2019

APPROVAL PAGE

This thesis is submitted in partial fulfillment of

the requirements for the degree of

Master of Science

Kristen E. Bachand

Approved by the Committee, August 2019

Romuald N. Lipcius, Ph.D.
Committee Chair / Advisor

Robert J. Orth, Ph.D.

Rochelle D. Seitz, Ph.D.

Jeffrey D. Shields, Ph.D.

TABLE OF CONTENTS

ACKNOWLEDGEMENTS

I would like to thank my advisor, Romuald Lipcius, and the rest of my committee, Rochelle Seitz, Jeffrey Shields, and Robert Orth for their advice and insight. They guided me to a project through long discussions, intriguing questions, and the bewildering field work conditions of 2018.

To the technicians of the Marine Conservation Ecology and Community Ecology Labs at VIMS, this project would not have been possible without you. I cant express my thanks enough to Katie Knick, Mike Seebo, Gabby Saluta, and Alison Smith. You helped me through numerous days in the field, whether the weather was beautiful or we ended up in Poquoson fleeing a thunderstorm. Then there were the many weeks spent in the lab looking for crabs in what felt like endless samples. If you hadnt been there, I would probably be still sorting.

To my fellow students, Kathy Longmire, Shantelle Landry, and Michelle Woods. Just having you in the lab to chat while I was endlessly searching for crabs made the time so much more enjoyable. Kathy, I enjoyed finding your sketches in my field notebook whenever you came out to help. Shantelle, I couldnt have gotten through nine bags in one day without you. Michelle, Im glad you enjoyed doing something a little bit different from your usual work.

I truly appreciate the advice from numerous people from the GIS User Group here at VIMS. David Wilcox, Erica Smith, Jessica Hendricks, Daniel Schatt, and other members of the group helped me through my first experience diving into raster data. Those key email and in-person conversations helped me immensely in devising my methods.

To all my fellow students here at VIMS, thank you for an amazing three years. From TGIs to fall and spring parties to chili cook-offs to impromptu group beach days, it has truly been a great experience.

None of this would have been possible without my funding sources. Special thanks to the Virginia Institute of Marine Science Academic Studies, Virginia Sea Grant, and the Willard A. Van Engel Fellowship.

Finally, to my parents and my twin sister, for being with me on this journey and being excited for every day I was out in the field when you were all stuck inside, either at work or preparing to be an awesome physical therapist. Even if the topic of my activities or complaints made little sense, you were always there. Especially to my parents, for their never-ending support even before they knew a career in marine science was possible for me. Thank you for all your love and encouragement over the years.

LIST OF TABLES

LIST OF FIGURES

ABSTRACT

To protect and manage ecosystems over large spatial scales, repeated mapping with remote sensing, such as aerial photography, is valuable, but several potential problems need to be overcome to generate accurate maps. For instance, to monitor submerged aquatic vegetation (SAV), such as seagrass, satellite imagery must often capture seasonal and inter-annual variation as well as disturbances. We used a model system, SAV and the blue crab *Callinectes sapidus* in the lower Chesapeake Bay, to examine (i) if Planet Lab (PL) satellite imagery can be used to accurately estimate SAV coverage by comparing PL images coincident with those of the VIMS SAV survey; (ii) if PL imagery can capture seasonal and episodic changes in SAV accurately; and (iii) if PL and VIMS SAV survey imagery can be integrated to assess the relationship between SAV nursery habitat and recruitment of young juvenile blue crabs in mid-summer through early fall. To do so, we analyzed data from six selected sites with high salinity in lower Chesapeake Bay. Our findings were (i) PL satellite imagery was a suitable surrogate for VIMS aerial surveys of SAV conducted annually at the selected sites, with the caveat that PL imagery is at a lower resolution (3 m) than the VIMS SAV survey (24 cm), which could affect the utility of PL imagery for some goals; (ii) PL imagery was able to capture seasonal and episodic changes in SAV cover in the Bay; and (iii) remote sensing imagery taken in late spring and early summer was not representative of SAV cover available to the blue crab during the recruitment period in mid-summer through fall. Consequently, PL imagery can be used to estimate SAV bed area over time scales that are relevant to recruitment of the blue crab in lower Chesapeake Bay.

Understanding SAV dynamics and future effects of climate change on SAV can be improved with broad-scale data from remote sensing techniques, such as aerial photography and satellite imagery. However, new platforms such as Planet Lab can provide accurate spatial and temporal distribution patterns for SAV beds relative to abundance of the blue crab during critical phases in its life history. At two locations in the York River, lower Chesapeake Bay, we conducted a mensurative field experiment by sampling percent cover of SAV (eelgrass *Zostera marina*, widgeon grass *Ruppia maritima*) and algae (mostly *Gracilaria vermiculophylla*), density of blue crab juveniles, bed area by Planet Lab, and select independent variables bimonthly over two years. The main findings were: (i) juvenile blue crab density was inversely related to SAV bed area, but reductions in crab density as bed area increased were more than offset by higher total abundance of crabs as bed area enlarged; (ii) crab density was positively related to percent cover of algae (*Gracilaria*), *Ruppia* and *Zostera*; (iii) location, year, season and water depth were not significant predictors of crab density in SAV beds after accounting for the effects of bed area and SAV percent cover; and (iv) potential loss of *Zostera* in the lower Chesapeake Bay due to global warming was projected to cause either only a modest reduction in crab density if other SAV species do not compensate and bed area remains constant, or crab density could even increase if algae and *Ruppia* were to compensate for the loss of *Zostera*.

Satellites, Seagrass, and Blue Crabs: Understanding Inter-Annual Fluctuations and Linkages in the York River

CHAPTER 1

USING SATELLITE IMAGERY TO TRACK CHANGES IN SUBMERGED AQUATIC VEGETATION WITHIN A COASTAL TEMPERATE ESTUARY

1.1 Introduction

Remote sensing techniques are more cost effective than field methods for surveying large areas (Mumby et al., 1999). One technique, aerial photography, has long been used to survey seagrass beds due to its high resolution, serving as a baseline for management efforts (Mumby et al., 1997; Ferwerda et al., 2007). The use of satellite imagery has gradually expanded to complement aerial photography (Dekker et al., 2006). When comparing maps from satellite imagery to those from aerial surveys, typically on the distribution and changes in extent of seagrass beds, there are few differences (Mumby et al., 1997; Howari et al., 2009; Roelfsema et al., 2009; Lyons et al., 2011; Meyer and Pu, 2012; Lathrop et al., 2014). One of the first satellites used was the Landsat Thematic Mapper (TM) with a spatial resolution of 30 m (Ferguson and Korfmacher, 1997; Roelfsema et al., 2009; Yang and Yang, 2009; Pu et al., 2010; Meyer and Pu, 2012). Using the Landsat TM, the presence or absence of seagrass and seagrass extent in St. Joseph Sound and Clearwater Harbor, Florida (USA), were determined with equivalent accuracy (71%) as aerial photointerpretation maps (Meyer and Pu, 2012). In coastal lagoons of North Carolina (USA), Landsat TM had an agreement as high as 73% with aerial images (Ferguson and Korfmacher, 1997). In general, coarse-detail mapping with satellite imagery is about 70% accurate, while fine-detail mapping is lower at about 40% (Mumby et al., 1999); nonetheless, satellite images have been useful in the determination of spatial and temporal dynamics of seagrass beds over large areas (Koedsin et al., 2016).

As technology has improved, satellites with higher spatial resolution than the Landsat

TM have been used. For instance, satellites such as the China Brazil Earth Resources Satellite and the Systeme Probatoire de l'Observation de la Terre (SPOT) with improved resolution at 20 m were used to detect seagrass (Mumby et al., 1997; Yang and Yang, 2009). The QuickBird and IKONOS satellites with 4-m spatial resolution further enhanced the utility of satellite images to map seagrass at even finer scales (Yang and Yang, 2009; Pu et al., 2010).

More recently, emphasis has shifted from simply mapping seagrass beds with satellite imagery to examining how seagrass distribution changes through time, with the Landsat TM images at low spatial resolution to the SPOT, IKONOS, and QuickBird images at high resolution (Dekker et al., 2005; Gullström et al., 2006; Barillé et al., 2010; Howari et al., 2009; Lyons et al., 2011, 2013). These studies have been able to determine if seagrass extent is declining (Dekker et al., 2005), increasing (Barillé et al., 2010; Howari et al., 2009), or remaining stable (Gullström et al., 2006; Lyons et al., 2011, 2013), which has been supported with complementary field observations (Howari et al., 2009; Lyons et al., 2011).

To protect and manage ecosystems, often over large spatial scales, repeated mapping with remote sensing can be a useful management tool since managers can track changes in the ecosystem over time (Mumby et al., 1999; Gullström et al., 2006). However, several potential problems need to be overcome to generate accurate maps (Roelfsema et al., 2013). To monitor submerged aquatic vegetation (SAV), such as seagrass, satellite imagery must capture seasonal variation and disturbance events, which requires a high image frequency on the order of hours to weeks (Roelfsema et al., 2013; Muller-Karger et al., 2018). Sometimes a given set of imagery may not be available for a particular time scale or time of year for a specific goal. For example, in Chesapeake Bay the blue crab recruits to SAV during mid-summer and early fall (Lipcius et al., 2007), a period not typically assessed by annual aerial surveys in the region (Orth and Moore, 1986). To understand the influence of SAV upon blue crab recruitment, remote sensing surveys of SAV would need to be undertaken

during that time period. Therefore, it may be necessary to combine data from different sources of imagery to determine the extent of SAV cover during periods when blue crabs recruit to their juvenile habitat. The overall goal of this study was to use a model system to investigate how newly available sources of imagery can be used to generate time series of SAV beds such as seagrass to investigate seasonal changes in cover over large spatial scales.

1.2 Model system: SAV and blue crab (*Callinectes sapidus*) in Chesapeake Bay

In Chesapeake Bay, the SAV Program at the Virginia Institute of Marine Science (VIMS) has conducted an aerial survey from May to October of each year for nearly four decades (Orth et al., 2017a,b, 2018). From May to July, the survey focuses on the lower Chesapeake Bay polyhaline and mesohaline SAV beds, and on the upper bay and its lower salinity tributaries from August to October (R. Orth, personal communication). Its goal is to determine the distribution of SAV beds within the bay system and inform ongoing restoration and management efforts directed at SAV species. When processing the aerial imagery, the VIMS SAV survey must account for tides, SAV growth stage and type (e.g. seagrass, macroalgae), water clarity, wind conditions, and cloud cover. The images are then used to create a comprehensive map with 24-cm resolution to assess inter-annual changes in SAV cover (Orth et al., 2017b, 2018).

The blue crab recruitment period spans July through November (mid-summer through fall) when young juveniles use the SAV beds in the lower Chesapeake Bay as nursery habitat (van Montfrans et al., 1990; Lipcius et al., 2007). Structured habitats such as seagrass and algal beds provide food and protection from predators for juvenile blue crabs and many other estuarine species (Heck and Thoman, 1984; Orth and van Montfrans, 1987; van Montfrans et al., 1990; Pardieck et al., 1999; Lipcius et al., 2005, 2007; Seitz et al., 2005, 2008; Johnston and Lipcius, 2012; Bromilow and Lipcius, 2017), as do other coastal habitats (i.e. oyster beds, salt marshes) for a range of fish and invertebrates (Barbier et al., 2011; Seitz

et al., 2014; Vasconcelos et al., 2014). Hence, analysis of aerial or satellite imagery of SAV beds over time relative to abundance of juvenile blue crabs may reveal the association between extent of nursery habitats, blue crab abundance, and ecosystem services (Anderson, 1989; Lefcheck et al., 2019). However, the VIMS SAV survey only focuses on SAV beds in high salinity regions within the lower Chesapeake Bay once per year, from May to July, and thus may not represent the available nursery habitat for juvenile blue crabs due to episodic disturbances and seasonal changes (Orth and Moore, 1986). In contrast, satellite imagery from Planet Lab, which has a large fleet of satellites (Planet Team, 2019), is taken throughout the year on a semi-weekly basis, potentially allowing the capture of monthly changes in cover, episodic events, and seasonal alterations.

The specific objectives of this study were to determine (i) if Planet Lab (PL) satellite imagery can be used to accurately estimate SAV coverage by comparing PL images coincident with those of the VIMS SAV survey; (ii) if PL imagery can capture seasonal and episodic changes in SAV accurately; and (iii) if PL and VIMS SAV survey imagery can be integrated to assess the relationship between SAV nursery habitat and recruitment of young juvenile blue crabs in mid-summer through early fall. These were accomplished by quantifying SAV cover using 2017 and 2018 PL imagery in tandem with aerial photographs from the VIMS SAV survey.

1.3 Methods

1.3.1 Field sites

Field sites were in the mainstem of the lower Chesapeake Bay and the York River (Figures 1.1 and 1.2). The lower bay sites corresponded to VIMS Juvenile Blue Crab Survey locations: Dameron Marsh, Occahanock, Pocomoke, and Poquoson (Figure 1.1). This survey runs from May through July each year, corresponding to peak SAV biomass, and supplements the Blue Crab Winter Dredge Survey (Sharov et al., 2003; Virginia Institute of Marine Science, 2018) by sampling shallow water sites. The York River sites were Al-

lens Island and the Goodwin Islands, selected as representative of a mixed bed of seagrass species and a mixed bed of algal and seagrass species, respectively (Figure 1.2). Allens Island consisted predominantly of seagrasses, eelgrass *Zostera marina* and widgeon grass *Ruppia maritima*. The Goodwin Islands had a well mixed bed with eelgrass and widgeon grass in addition to *Gracilaria vermiculophylla* and some woody and leaf debris (Wood, 2017). *Gracilaria vermiculophylla* often does not remain anchored to the bottom and can be moved by tides, currents, and storm conditions, resulting in frequent changes to the viewable bed area in remote sensing imagery (Thomsen et al., 2007). All field sites were shallow, between 0.3 and 1.2 m deep at low tide. Salinity ranged from 10 to 20 depending on precipitation and local conditions.

1.3.2 Imagery selection

Visible color images for 2017 from all six sites were used to compare the VIMS SAV survey and PL imagery, focusing on the above-ground SAV visible to the unaided eye in both imagery sources. The imagery sources had differing resolutions, with the VIMS SAV survey at 24-cm resolution and PL imagery at 3-m resolution. The selected images needed to have no or minimal cloud cover, which can be a challenge when working with remote sensing images (Mumby et al., 1997; Koedsin et al., 2016). Water clarity was considered good if tidal height was low and if known sand bars or shoals were visible, metrics also used by the VIMS SAV survey to define usable images (D. Wilcox, personal communication). Images were matched as close as possible temporally, but no more than two days apart (Table 1.1). Only the York River sites (Allens Island and the Goodwin Islands) were examined for the time series analysis. PL images were selected from May to November in 2017 and 2018, with two images per month when possible.

1.3.3 Analysis of remote sensing imagery

ArcMap 10.4 (ESRI, 2015) was used to calculate percent agreement between VIMS SAV survey and PL imagery. For the lower Chesapeake Bay sites, polygons were drawn around the 2017 Juvenile Blue Crab Survey sites. For the York River sites, the images from the 2016 VIMS SAV survey were used to search for local SAV beds, but polygons were drawn based on field observations and scaled to match concurrent blue crab sampling efforts. Each polygon encompassed areas known to contain seagrass, which was mapped in ArcMap, but were expanded to include unvegetated areas (Table 1.2) to compare the ability of the PL and VIMS SAV survey imagery to detect SAV. Thirty random points were generated within each polygon at each site, specified to be at least 10 m apart (Figure 1.3). The presence or absence of SAV was used to calculate the percent agreement between the imagery types, based on whether the images agreed or disagreed on the occurrence of SAV.

For the time series analysis, PL images from the York River for 2017 and 2018 (Table 1.3) were classified using Interactive Supervised Classification, with no more than eight pixel classes per image for ease of interpretation (K.E.B, personal observation). Pixel classes represented the color of the terrestrial area, unvegetated bottom, and the varying shades of SAV present. Each classified image was then converted into a polygon and used to manually outline the visible SAV beds. Each polygon's area was then calculated through the Calculate Geometry function in ArcMap and visualized using R Studio (ESRI, 2015; RStudio Team, 2016).

1.4 Results

1.4.1 Field site conditions

Water quality differed slightly between the two sampling years (Table 1.4). The watershed received 20 to 25 cm of rainfall during July 2018 in comparison to 5 to 10 cm in July 2017 (National Weather Service, 2019). This caused the salinity at the two study sites to

be uncharacteristically low in 2018, despite a similar trend over time (Figure 1.4). Mean salinity in 2017 remained between 19.1 and 21.6, which is typical for the York River. However in 2018, salinity was on average below 20 for the entirety of sampling, with values as low as 14.1. The heightened precipitation also increased turbidity, particularly in July, with a mean value of 44.1 NTU (Figure 1.5, Table 1.4). As a result, water clarity decreased, making it hard to find usable satellite images during the summer months and sample SAV in the field. Water temperature varied seasonally, but did not vary significantly between 2017 and 2018 (Figure 1.6).

1.4.2 Validation of PL imagery as a surrogate for aerial imagery

For the lower Chesapeake Bay and York River sites in 2017, the mean percent agreement between PL and VIMS SAV survey imagery was 91.1% with a margin of error of $\pm$5.3% (Table 1.5). Values ranged from 80.0% at Pocomoke to 100.0% at Dameron Marsh. Interestingly, correspondence at the western shore sites (93.3% and 100%) was significantly better than at the eastern shore sites (80.0% and 90.0%; Tables 1.6 and 1.7). Whether a site was in the northern (Dameron Marsh, Pocomoke) or southern (Occahanock, Poquoson) locations did not influence correspondence (Tables 1.6 and 1.7). Moreover, correspondence did not differ between Allens Island and Goodwin Islands (Logistic regression, df = 1, 58, z = 0.46, p = 0.64). In addition, correspondence (Table 1.5) and percent SAV (Table 1.2) were not significantly correlated (Linear regression, df = 1, 4, r^2 = 0.03, p = 0.74). The association between correspondence and SAV bed area (Table 1.2) was marginally significant (Linear regression, df = 1, 4, r^2 = 0.57, p = 0.0502), but the correlation was driven by a single outlier (Pocomoke). After removing the outlier, correspondence and SAV bed area were also not significantly correlated (Linear regression, df = 1, 3, r^2 = 0.0003, p = 0.98). Finally, correspondence and polygon area (Table 1.2) did not correlate significantly (Linear regression, df = 1, 4, r^2 = 0.01, p = 0.88). Using the selection criteria for the SAV beds, PL imagery was validated as a surrogate for VIMS SAV survey imagery.

1.4.3 Temporal patterns in SAV captured by PL imagery

In 2017, trends in SAV bed area at Allens Island and the Goodwin Islands differed over time (Table 1.3; Figure 1.7). Allens Island had a peak in SAV bed area around 5 ha in July, and remained stable between 2.8 and 3.8 ha for the rest of the time series. In contrast, the Goodwin Islands peaked in late June around 3.8 to 5.7 ha, but declined sharply to 1.2 ha in August, most likely due to a tropical storm that passed the mouth of Chesapeake Bay on August 28 and 29. Bed area then fluctuated between 1.6 and 3.2 ha for the rest of the time series.

In 2018, the bed area trends between Allens Island and the Goodwin Islands were similar but temporally asynchronous (Table 1.3; Figure 1.7). Allens Island reached its peak in late June at just under 4.0 ha, then declined sharply to 0.84 ha by August. Thereafter, bed area continued to decrease slowly, dropping to 0.04 ha by November. From the start of the time series to the end, the bed area at Allens Island decreased by 99.1% (Figure 1.8). Conversely, the Goodwin Islands peaked at 3.7 ha in August, then more gradually declined to 0.13 ha by early November, with a slight recovery to 0.44 ha. By the end of the time series in 2018, the Goodwin Islands bed area declined by 74.6%, a less steep loss than Allens Island.

Satellite data on SAV bed area captured the change in SAV cover from spring and summer in the lower Chesapeake Bay to the SAV available to blue crabs during recruitment in the mid-summer and fall months, although this varied slightly based on site. On 1 June 2017, Allens Island had a bed area of 3.3 ha and the Goodwin Islands had 3.7 ha (Figure 1.7). By November 3, the Goodwin Islands had declined to 1.33 ha whereas Allens Island remained stable at 3.3 ha. On 20 June 2018, Allens Island began with 3.9 ha and the Goodwin Islands with 2.7 ha. After the seagrass die-off event, Allens Island declined to 0.03 ha and the Goodwin Islands to 0.44 ha (Figure 1.7).

1.5 Discussion

Using a model system of submerged aquatic vegetation (SAV) and blue crab recruitment in the lower Chesapeake Bay, our specific findings were (i) Planet Lab (PL) satellite imagery was a suitable surrogate for VIMS aerial surveys of SAV conducted annually at the surveyed sites, with the caveat that PL imagery is at a lower resolution (3 m) than the VIMS SAV survey (24 cm), which could affect the utility of PL imagery for some goals; (ii) PL imagery was able to capture seasonal and episodic changes in SAV cover in the Bay; and (iii) a remote sensing image taken in late spring and early summer was not representative of SAV cover available to the blue crab during the recruitment period in late summer through fall. Consequently, PL imagery can be used to estimate SAV bed area over time scales that are relevant to recruitment of the blue crab in the lower Chesapeake Bay.

The correspondence of PL satellite imagery with aerial imagery from the VIMS SAV Survey was very high, ranging from 80.0% to 100.0% in lower Chesapeake Bay sites and 90.0% to 93.3% in York River sites. The comparability of the two image types was well above the typical benchmark of 40% for fine-scale mapping with satellite imagery (Mumby et al., 1999). The high correspondence could be reduced if images are unavailable with good water clarity, low cloud cover, and known SAV presence. Some variation in correspondence was evident between the western and eastern shores of Chesapeake Bay; correspondence was higher at western shore sites (Dameron Marsh, Poquoson), which ranged from 93.3% to 100.0%, than at eastern shore sites (Pocomoke and Occahanock), which ranged from 80.0% to 90.0%. In addition, correspondence at two closely spaced locations, Allens Island and Goodwin Islands, was high (90.0% and 93.3%, respectively) and did not differ by location.

PL imagery successfully captured seasonal and episodic events. In 2017, there were no extreme weather events or conditions, reflected in a relatively constant SAV cover at Allens Island throughout the year. However in 2018, there was twice as much rainfall resulting in

lower salinity and increased turbidity. The negative effect on SAV cover was reflected in the PL imagery at the York River, with severe changes at Allens Island. In addition, the impact of an episodic event, a tropical storm, was captured in August 2017 at the Goodwin Islands due to shifting algal cover not present at Allens Island (K.E.B, personal observation).

Remote sensing imagery taken in the spring at the height of SAV coverage did not represent the decline in SAV cover in the fall when juvenile blue crabs recruit to this habitat. SAV cover was highly variable over the course of a year due to weather patterns, seasonal variation, and episodic disturbances. Only the imagery from Allens Island could be applicable at any time in 2017, but this was the exception. The Goodwin Islands were affected by a tropical storm in 2017 and both sites were affected by high precipitation in 2018, which presumably led to the decrease in SAV cover. The temporal variation on a seasonal scale was too high to successfully use a spring image for fall SAV cover. Thus, we verify that snapshot imagery surveys may be representative of a specific time period, but not of intra-annual variation.

We also examined whether the percent cover of SAV in a polygon, SAV bed area, and polygon area of an image influenced correspondence between VIMS SAV survey and PL imagery. Neither percent cover of SAV (r^2 = 0.03) nor polygon area (r^2 = 0.01) affected correspondence, even though percent cover and polygon area ranged widely, from 8.6% to 57.1% for percent cover and from 14.5 to 1023.0 ha for polygon area. Correspondence was marginally correlated with SAV bed area (r^2 = 0.57, p = 0.0502), but this was due to a single outlier. After removing the outlier, correspondence was not associated with SAV bed area (r^2 = 0.0003). Despite these findings, we encourage others to examine these possible sources of bias, specifically that the degree of correspondence may be affected by percent cover of SAV, SAV bed area, or polygon area in an image. For example, if images have extremely low percent cover, correspondence could be higher if detection of unvegetated habitat were more accurate than that for vegetated habitat.

This study communicates the importance of remote sensing imagery captured and pro-

cessed on a regular basis to inform long-term monitoring efforts. Many surveys used in conservation monitoring are only done once per year. They can miss important seasonal and episodic changes that may impact the monitored ecosystem. Using regularly taken satellite imagery can capture disturbance events in real time, whereas a yearly survey can only capture the end result and miss changes over time.

Researchers can utilize the different characteristics of imagery sources to examine complex questions. Hyperspectral imagery can examine SAV traits usually measured in field surveys, such as biomass, blade length, and shoot density (Lathrop et al., 2014; Koedsin et al., 2016). Multiple remote sensing sources often have different spatial resolutions ranging from sub-meter to 30 m, which can be used to address different questions (Yang and Yang, 2009; Orth et al., 2017a, 2018). Finer spatial resolutions are recommended, since they can examine SAV at finer scales (Muller-Karger et al., 2018) and improve understanding of bed boundaries which can vary based on the bed type or substrate (Mumby et al., 1997; Meyer and Pu, 2012). Imagery sources can have differing frequencies of image capture, from hours and days to months and years (Muller-Karger et al., 2018). Combining these images can capture events on different time scales and make it possible to examine the impacts of seasonal variation and episodic events. Differing imaging frequencies from multiple sources could potentially account for cloud cover and water clarity, which are impossible to control (Mumby et al., 1997; Koedsin et al., 2016). Fusing annual remote sensing surveys with additional sources can address knowledge gaps about changes in SAV cover on a fine scale, and how these changes may affect recruitment of the various species that use SAV beds as nursery habitats. This can encompass varying temporal and spatial scales, ranging from local weather events to climate change, and help resource managers prepare for future environmental change.

Tables

Table 1.1: Date of image selection for the VIMS SAV Survey and Planet Lab imagery in 2017 (listed alphabetically).

Location	SAV Survey	Planet Lab
Allens Islands	June 29	June 29
Dameron Marsh	July 9	July 9
Goodwin Islands	June 29	June 29
Occahanock	May 17	May 16
Pocomoke	June 12	June 14
Poquoson	June 29	June 29

Table 1.2: Area of the polygons used for comparison study at the six lower Chesapeake Bay sites. The area of the SAV bed, in hectares, was outlined by eye using Planet Lab imagery at each location. The comparison polygons were determined based on the VIMS Juvenile Blue Crab Survey and field observations. Percent SAV is the percent of the comparison polygon that contains by SAV.

Location	SAV Bed (ha)	Comparison Polygon (ha)	Percent SAV
Allens Islands	5.9	16.6	35.5%
Dameron Marsh	44.1	296.9	14.9%
Goodwin Islands	6.5	14.5	44.8%
Occahanock	88.2	1023.0	8.6%
Pocomoke	292.4	787.4	37.1%
Poquoson	188.6	330.1	57.1%

Table 1.3: Date of image selection for the time series of Planet Lab imagery. The same image was used for both Allens Island and the Goodwin Islands.

2017		2018	
Date	Day of Year	Date	Day of Year
June 1	152	May 12	132
June 29	180	May 24	144
July 19	200	June 20	171
July 31	212	July 10	191
August 31	243	August 6	218
September 24	267	August 25	237
October 3	276	September 5	248
October 18	291	October 1	274
November 3	307	November 4	308
November 17	321	November 16	320

Table 1.4: Water quality parameters at the Goodwin Islands Continuous Monitoring Station (CHE019.38) from May to November in 2017 and 2018. Data are from the Virginia Estuarine and Coastal Observing System (VECOS) network operated by the Chesapeake Bay National Estuarine Research Reserve (CBNERR) at VIMS. Presented is the mean per month of each parameter.

	2017			2018		
	Temperature (°C)	Salinity	Turbidity (NTU)	Temperature (°C)	Salinity	Turbidity (NTU)
May	20.1	19.4	10.4	21.8	17.5	5.8
June	25.2	19.1	8.5	26.6	14.1	8.5
July	28.2	20.8	5.6	27.8	16.1	44.1
August	27.0	20.6	12.6	28.6	16.5	12.3
September	24.1	19.9	15.9	27.4	15.2	13.8
October	21.0	20.2	5.9	21.0	14.5	8.4
November	13.6	21.6	5.0	12.7	14.4	5.0

Table 1.5: Correlation between SAV survey aerial and PL satellite imagery in 2017 for absence/presence of SAV. Values represent the mean ±margin of error. Each image had 30 sampling points. The percent correlation reflects the percentage of comparison points that matched.

Location	Percent correlation
Allens Islands	90.0 ± 17.3%
Dameron Marsh	100.0 ± 11.4%
Goodwin Islands	93.3 ± 15.6%
Occahanock	90.0 ± 17.3%
Pocomoke	80.0 ± 21.6%
Poquoson	93.3 ± 15.6%
Mean Agreement ± (SE)	91.1 ± 5.6%

Table 1.6: AIC calculations for correspondence between PL satellite and SAV survey aerial imagery. k = number of parameters, including sample variance (s^2) as a parameter. AIC_c = corrected AIC value. Δ_i = difference between model g_i and the best model. w_i = model probability of fitting the observed data. Model g_3 with two factors was not significantly better than model g_1 with only one factor (Likelihood ratio χ^2 test, df = 118, p = 0.75).

Model	Variables	k	AIC_c	Δ_i	w_i
g_1	Shore	3	72.47	0	0.70
g_2	Latitude	3	77.43	5.17	0.05
g_3	Shore + Latitude	4	74.51	2.04	0.25

Table 1.7: Estimate, SE (standard error), and 95% Confidence Interval (CI) of the parameters from logistic regression model g_1 from Table 1.6.

Parameter	Variable	Estimate	SE	95% CI	p
α	Intercept	1.74	0.36	(1.01, 2.46)	$<<$0.0001
β	Shore	1.63	0.81	(0.02, 3.24)	$<$0.043

Figures

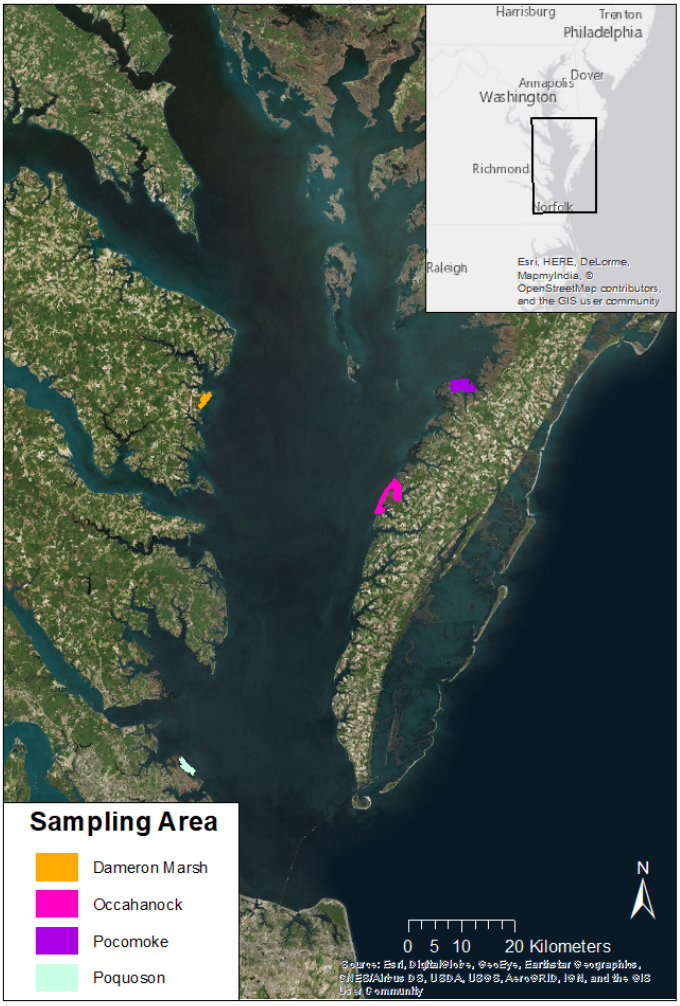

Figure 1.1: Locations of the four VIMS Juvenile Blue Crab Survey sampling sites within the lower Chesapeake Bay; see Ralph et al. (2013) for details of the survey. The colored areas were used in the assessment of accuracy of Planet Lab remote sensing imagery.

Figure 1.2: Locations of the two sampling sites within the York River, Allens Island and the Goodwin Islands. The colored portion represents the area used for the remote sensing technique comparison.

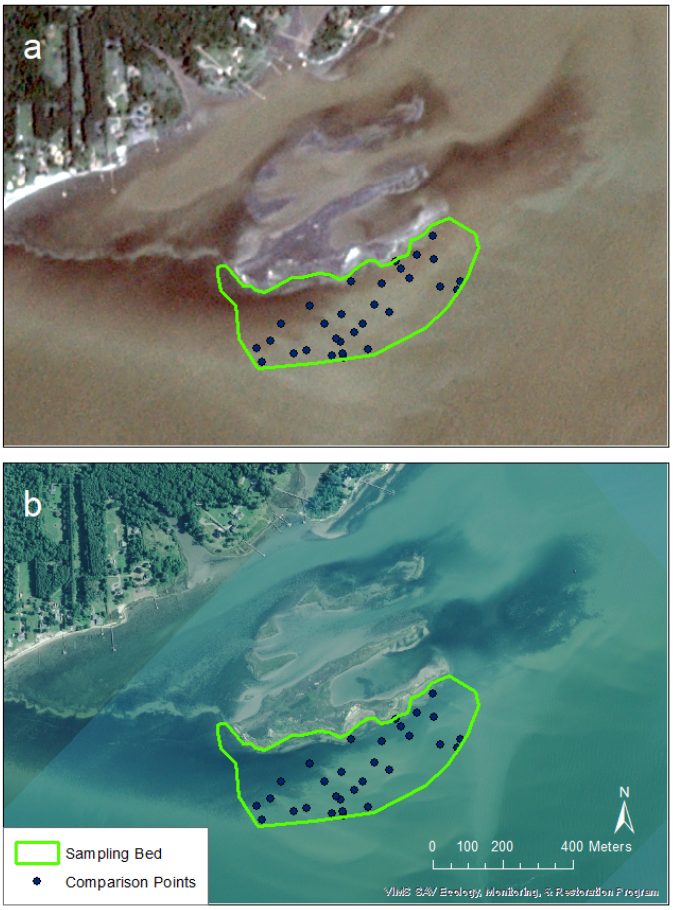

Figure 1.3: Example of the Planet Lab (a) and VIMS SAV survey (b) imagery comparison. Pictured is Allens Island on June 29, 2017.

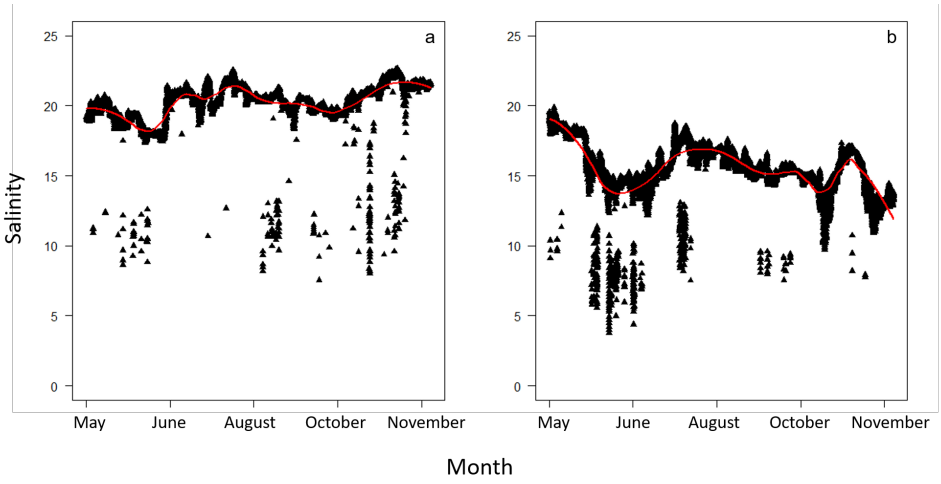

Figure 1.4: Salinity at the Goodwin Islands Continuous Monitoring Station (CHE019.38) from May to November in 2017 (a) and 2018 (b). Data are from the Virginia Estuarine and Coastal Observing System (VECOS) network operated by the Chesapeake Bay National Estuarine Research Reserve (CBNERR) at VIMS. The red line represents a loess fit (span = 0.25).

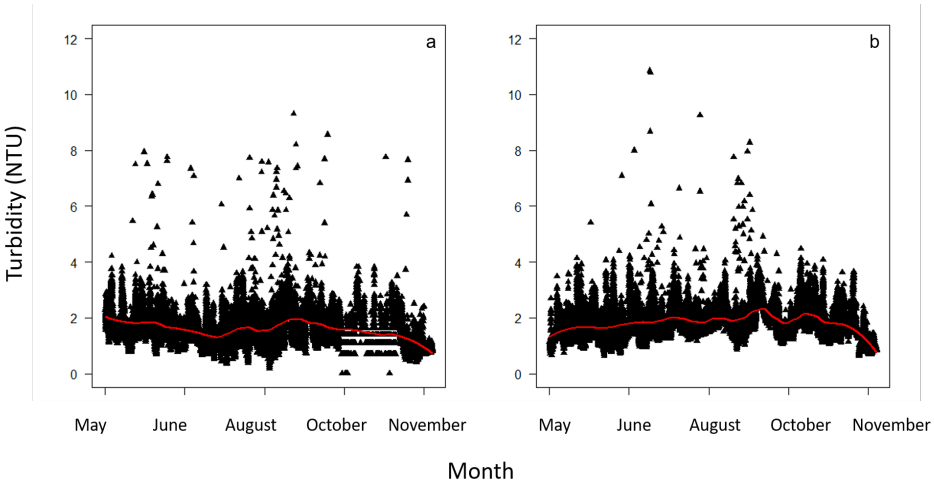

Figure 1.5: Turbidity at the Goodwin Islands Continuous Monitoring Station from May to November in 2017 (a) and 2018 (b). Data are from the VECOS Network operated by the CBNERR at VIMS. The red line represents a loess fit (span = 0.25).

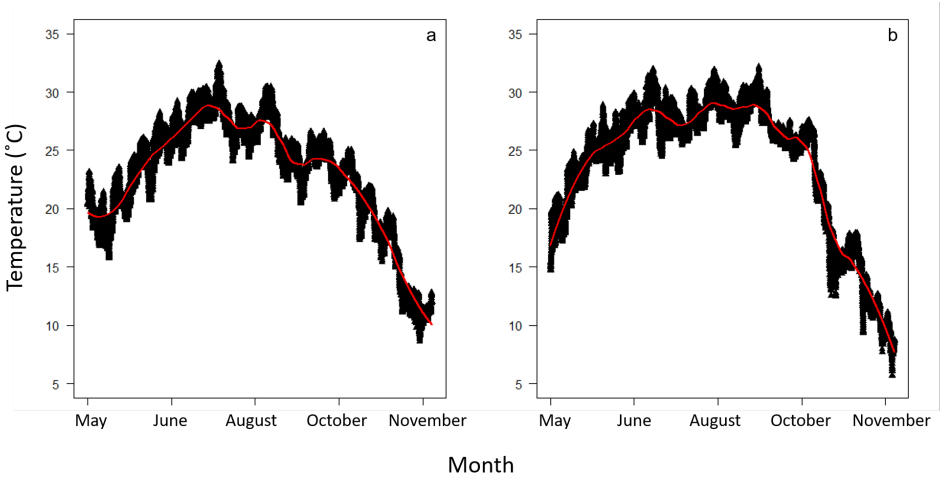

Figure 1.6: Water temperature at the Goodwin Islands Continuous Monitoring Station from May to November in 2017 (a) and 2018 (b). Data are from the VECOS Network operated by the CBNERR at VIMS. The red line represents a loess fit (span = 0.25).

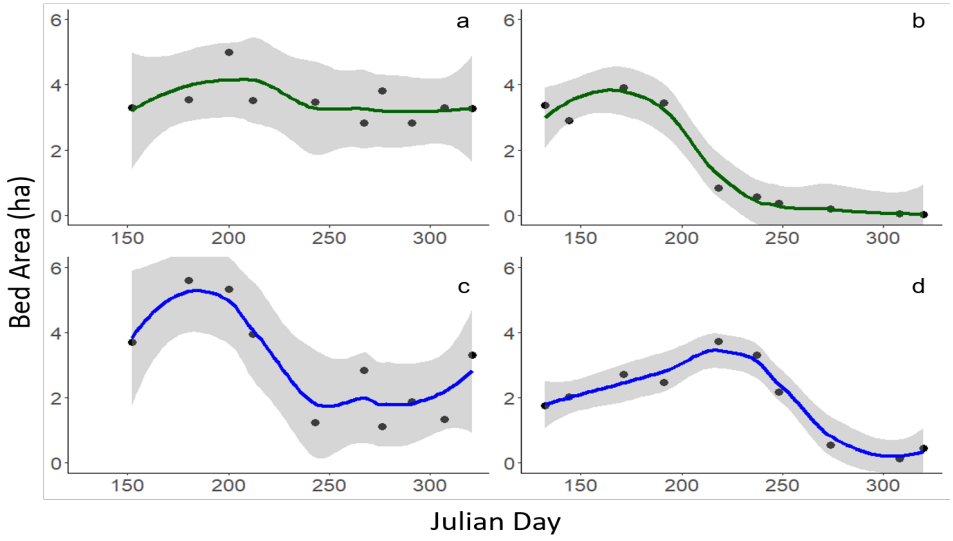

Figure 1.7: Trends in SAV bed area at Allens Island (dark green) in 2017 (a) and 2018 (b), and the Goodwin Islands (dark blue) in 2017 (c) and 2018 (d), calculated using Planet Lab satellite imagery. The time series runs from May to November in both years. The colored line represents the loess fit (span = 0.75). The dark grey areas represent 95% confidence intervals, calculated based on the fit of the data to the loess line.

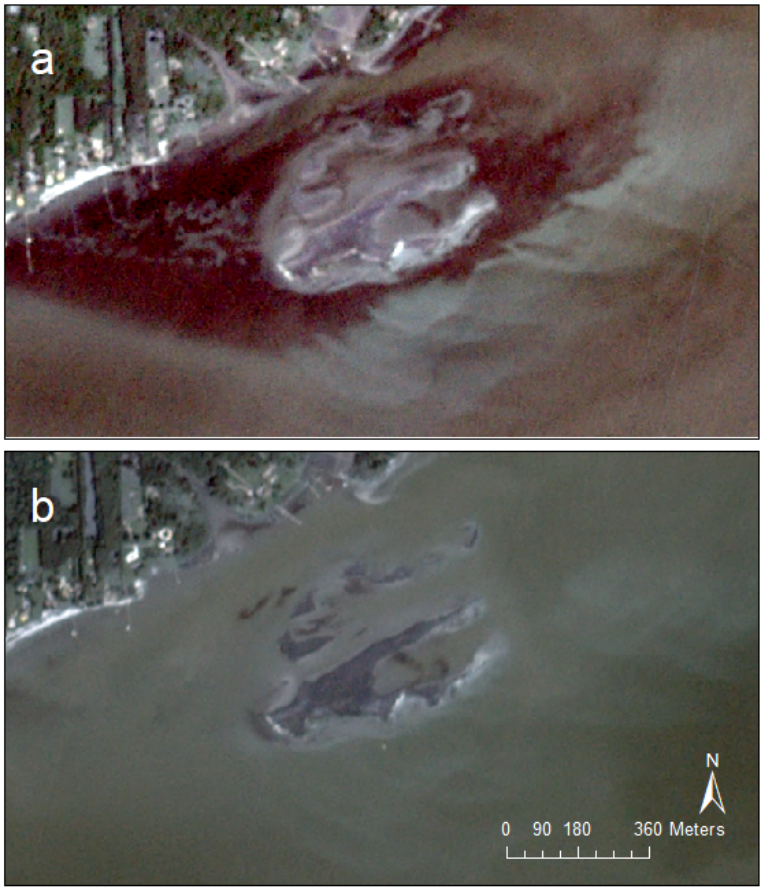

Figure 1.8: A depiction of a loss of seagrass cover at Allens Island in the York River over the summer of 2018. Notice the decrease from May 24 (a) to September 5 (b).

CHAPTER 2
IMPACT OF VARIATION IN SUBMERGED AQUATIC VEGETATION AND CLIMATE CHANGE ON JUVENILE BLUE CRABS IN NURSERY HABITATS OF CHESAPEAKE BAY

2.1 Introduction

Many ecologically and commercially valuable marine and estuarine species, including the blue crab *Callinectes sapidus*, depend on structured nursery habitats, such as seagrass beds, salt marshes and mangrove forests (Beck et al., 2001; Heck et al., 2003; Boström et al., 2006; Seitz et al., 2014). Much is known about the influence of patch characteristics of nursery habitats on survival, abundance and growth of juveniles of the blue crab and various other fish and crustaceans (Hovel and Lipcius, 2001, 2002; Lipcius et al., 2007; Seitz et al., 2014). For instance, variation in seagrass patch size, due to habitat fragmentation, alters blue crab survival, which is inversely related to patch size due to the association of larger, cannibalistic blue crabs with large patches (Hovel and Lipcius, 2001). In addition, the value of seagrass patches varies seasonally and with habitat complexity (Hovel and Lipcius, 2001). As fragmentation increases, the distance between the patches increases, decreasing the connectivity of the landscape and creating more unvegetated and unstructured habitat in which juvenile blue crabs suffer high mortality (Lipcius et al., 2007). In contrast to such examples of patch-related effects, little information exists on the broad-scale effects of nursery habitat on the demography of fish and crustaceans (Ralph et al., 2013; Lipcius et al., 2019). In part this has been due to logistical limitations associated with acquisition of broad-scale data on habitat availability over time by techniques such as aerial or satellite imagery (Mumby et al., 1997, 1999; Howari et al., 2009; Roelfsema et al., 2009; Lyons et al., 2011; Meyer and Pu, 2012; Lathrop et al., 2014). Recently, however, new platforms

such as Planet Lab have facilitated acquisition of satellite imagery at sufficient resolution to quantify accurate temporal patterns of habitat distribution, such as seagrass beds (Chapter 1).

The blue crab has served as a model system for investigating the characteristics of nursery habitats that drive population dynamics in marine crustaceans (Hines, 2007; Lipcius et al., 2007; Seitz et al., 2014; Lipcius et al., 2019). Young juvenile blue crabs inhabit shallow, structured nursery habitats such as seagrass and macroalgal beds, salt marshes, and coarse woody debris (Heck and Thoman, 1984; Orth and van Montfrans, 1987; Wilson et al., 1990; Everett and Ruiz, 1993; Hines and Ruiz, 1995; Lipcius et al., 2007), which provide food and refuge (Perkins-Visser et al., 1996; Pile et al., 1996; Hovel and Lipcius, 2001; Lipcius et al., 2005; Seitz et al., 2005; Johnston and Lipcius, 2012; Bromilow and Lipcius, 2017). Once juvenile crabs reach approximately 20-30 mm carapace width (CW), they attain a size refuge from most predators and then disperse to unstructured secondary nursery habitats (Lipcius et al., 2005; Seitz et al., 2005; Lipcius et al., 2007; Bromilow and Lipcius, 2017). Juvenile crab densities are highest in continuous seagrass beds and very small patches, when compared with moderately sized and large patches (Hovel and Lipcius, 2002). Juvenile crab density is also positively related to seagrass shoot density and vegetation percent cover (Hovel and Lipcius, 2002), which can vary based on year and location (Ralph et al., 2013).

Seagrass cover and distribution vary seasonally and interannually (Orth and Moore, 1986), and are likely to be altered further with climate change (Moore and Jarvis, 2008; Hines et al., 2010). Such variability may strongly influence blue crab recruitment. For instance, Stockhausen and Lipcius (2003) examined how juvenile blue crab recruitment might change if SAV beds were not available in the lower York River estuary. With most crabs settling in the lower Chesapeake Bay near the mouth of the York River, the effects of seagrass loss upriver were alleviated (Stockhausen and Lipcius, 2003). However, if this habitat were to disappear due to climate change, juvenile blue crabs could experi-

ence increased mortality when settling in unstructured habitats (Lipcius et al., 2007; Hines et al., 2010). Given the scarcity of information on the broad-scale effects of nursery habitat quantity and quality, we conducted a mensurative field experiment to examine the role of submerged aquatic vegetation (SAV) nursery bed area on abundance of blue crab juveniles relative to broad- and patch-scale features including percent cover of seagrass and algae, SAV bed area, water depth, location, season, and year. This study was facilitated by the recent demonstration that Planet Lab satellite imagery can provide accurate temporal distribution patterns of SAV relative to the seasonal recruitment window of the blue crab in nursery habitats (Chapter 1).

2.2 Logical framework and objectives

The specific goals of this study were to (i) examine the hypothesis that juvenile blue crab density in SAV nursery habitats is inversely related to bed area; (ii) evaluate alternative hypotheses concerning effects of SAV percent cover and other independent variables on juvenile blue crab density; and (iii) simulate potential effects of climate change on SAV nursery habitats and blue crab recruitment. We generated hypotheses (H_i) with varying combinations of algae (mostly *Gracilaria vermiculophylla*, see Wood (2017)) percent cover, widgeon grass *Ruppia maritima* (hereafter, *Ruppia*) percent cover, eelgrass *Zostera marina* (hereafter, *Zostera*) percent cover, bed area, year (2017, 2018), location (Allens Island, Goodwin Islands), Julian day, and water depth. Each H_i was associated with a specific statistical model g_i (Table 2.1), suited to the collected data. The suite of statistical models (g_i) represented multiple alternative hypotheses (Chamberlin, 1890) that were evaluated following an Information Theoretic approach (Burnham and Anderson, 2002; Anderson, 2008). For example, in H_1 (statistical model g_1), we expect juvenile blue crab density to correlate positively with total percent cover (Ralph et al., 2013), which includes all types of SAV. We also propose, as a null hypothesis, that greater bed area will be associated with lower juvenile blue crab densities, since crabs can disperse to other seagrass beds due to

density-dependent emigration (Pile et al., 1996), which is represented by H_2 and statistical model g_2. We expect juvenile blue crab density to correlate positively with percent cover of seagrass (i.e., *Ruppia* and *Zostera*), as seagrass is the preferred nursery habitat (Orth and van Montfrans, 1987; Lipcius et al., 2007; Seitz et al., 2008). Density of juvenile blue crabs could also correlate positively with algal percent cover, which serves as an alternative nursery habitat (Johnston and Lipcius, 2012; Wood, 2017). The remaining hypotheses and corresponding statistical models dealt with various combinations of independent factors and variables (Table 2.1).

2.3 Methods

2.3.1 Field sites

Field sites were in the York River at two locations, Allens Island and the Goodwin Islands (Figure 2.1). Sampling periods varied slightly for each year. In 2017, sampling was from August through November and in 2018 from June through October (Table 2.2). The extension in the time period for 2018 was designed to encompass the entire juvenile blue crab recruitment period. The sampling sites at each location were defined by past observations of the presence of seagrass and by the Virginia Institute of Marine Science (VIMS) SAV survey, defined by the comparison polygons in Chapter 1 (see Table 1.2 for Allens Island and the Goodwin Islands). Random sites were designated 10 m apart were assigned within each location, four sites per location in 2017 and 10 sites per location in 2018. The specific sampling plot of each site was adjusted in the field based on the presence or absence of SAV by selecting the next random site from a previously generated list.

2.3.2 Field sampling

At each site, a 1.68 m^2 drop net was deployed from the bow of the boat, ensuring any blue crabs present would be trapped within (Ralph et al., 2013). Water quality measurements (i.e., temperature, salinity, dissolved oxygen, depth) were taken per location in 2017 and

per site in 2018. Different parameters of SAV were measured within the drop net. Percent cover was estimated by species for seagrass (*Zostera* and *Ruppia*) and for algae (*Gracilaria* spp.). Absolute percent cover was calculated after sampling and used for the analysis. In 2018, a 12-cm core sample was taken for shoot density at one core-length from the seam on the drop net. All cores were taken back to the lab to determine shoot density by species. Samples were collected by suction for 6 min, which is 80% efficient in collecting the blue crabs present, followed by a sweep with a dip net to catch any remaining crabs (R. Lipcius, unpubl. data, Ralph et al. (2013)). Captured adult blue crabs were measured and sexed in the field and released. Suction samples were sorted for juvenile blue crabs, which were sexed if the carapace width was greater than 15 mm.

2.3.3 Satellite imagery analysis

Planet Lab satellite images, with 3-m resolution (Planet Team, 2019), were selected from June through November of 2017 and 2018 at Allens Island and the Goodwin Islands (Table 2.2). Images were selected based on their having no clouds and good water clarity for optimum visibility of SAV. Images were also within one to two weeks of the date of field sampling, which ensured the bed area captured in the image would align with field observations. Bed area was calculated using the Supervised Interactive Classification in ArcMap 10.4, based on the area of visible SAV per site in each image (ESRI, 2015).

2.3.4 Statistical analysis

All statistical analyses were performed in R Studio (RStudio Team, 2016) using a generalized linear model with the negative binomial distribution in the MASS package, which is ideal for analyzing count data that are overdispersed (Venables et al., 2002). The response variable was crab density from each of the samples. After running each of the statistical models (Table 2.1), the resulting Akaike Information Criterion (AIC) values from each model were used to calculate AICc, a second-order bias correction estimator (Anderson,

2008). Model probabilities (w_i) based on Δ_i values were used to rank the different models against the model with the lowest AICc. Any model with $w_i < 0.10$ was eliminated. Competing models were compared with likelihood ratio χ^2 tests (Vuong, 1989).

2.4 Results

2.4.1 Water Quality Parameters

In 2017, water temperature followed a seasonal trend, peaking in August at 28.0°C and declining to 12.6°C by November (Table 2.3). Salinity ranged from 20.7 to 23.1 throughout the sampling period. Dissolved oxygen varied greatly, fluctuating between 4.5 to 14.2 mg/L. Samples were taken in 0.7 to 1.2 m water depths. In 2018, water temperature followed the same seasonal trend, but at slightly warmer temperatures, with a peak at 31.2°C decreasing to 15.0°C by November (Table 2.4). Salinity was below 20 for the entire sampling period, fluctuating between 11.3 and 16.0. Dissolved oxygen was slightly lower, between 4.3 and 7.7 mg/L. Samples were also taken in shallower water as the sampling progressed through the summer, starting at 1.0 m but decreasing to 0.5 m due to the seagrass die-off in deeper water, which forced sampling farther inshore.

2.4.2 Blue crab recruitment, SAV bed area, and SAV percent cover

Multiple cohorts of juvenile blue crabs recruited in both 2017 (Figure 2.2) and 2018 (Figure 2.3). In addition, SAV bed area in Allens Island and the Goodwin Islands varied more than an order of magnitude seasonally and inter-annually in 2017 and 2018 (Figure 2.4). Given the presence and variation of juvenile blue crabs and SAV bed area, we were able to conduct our mensurative field experiment as planned to determine the relative influence of SAV bed area and patch-scale features of SAV on blue crab abundance in nursery habitats.

Crab density varied substantially between locations and years, ranging over two orders of magnitude, with highest densities reaching 100 per 1.68 m^2 (Figure 2.5), which equals about 60 m^{-2}. Percent cover of algae varied from 0% to 100% and was generally higher

at the Goodwin Islands than at Allens Island (Figure 2.6). Percent cover of *Ruppia* and *Zostera* varied from 0% to 100% and was generally higher at Allens Island (Figures 2.7 and 2.8). However, *Zostera* declined drastically and almost disappeared completely at both sites in 2018 (Figure 2.8).

2.4.3 Effects of SAV bed area and patch features on crab density

Of the 14 statistical models, only models g_4, g_6, g_7 and g_{11} were supported by the field data (Table 2.1). Seagrass shoot density was included in initial model runs, but was not a significant predictor and was excluded from the analysis. Model g_6, with independent variables SAV bed area and percent cover of algae, *Ruppia* and *Zostera*, had the highest weighted probability (w_6 = 0.54). Although models g_7 and g_{11} had more parameters than model g_6, they did not improve the fit to the data over model g_6 (likelihood ratio χ^2 tests, $p > 0.4$). In contrast, model g_6 fit the data significantly better than model g_4, which had fewer parameters (likelihood ratio χ^2 test, p = 0.035).

All independent variables within model g_6 were significantly different from 0 (Table 2.5). Blue crab density increased significantly with percent cover of algae, *Ruppia* and *Zostera* (Figure 2.9). In contrast, crab density was inversely related to bed area (Figure 2.9). The final equation for crab density from model g_6 (Table 2.5) is:

$$Density = e^{2.537+0.0317x_1+0.0213x_2+0.0109x_3-0.0000087x_4} \tag{2.1}$$

where x_1 = algal % cover, x_2 = *Ruppia* % cover, x_3 = *Zostera* % cover, and x_4 = bed area in m^2.

2.4.4 Simulated scenarios of SAV and crab density

To illustrate the relative effects of each independent variable on crab density, we used equation 2.1 to calculate crab density under various scenarios of bed area and percent cover

of algae, *Ruppia*, and *Zostera* (Table 2.6). In the reference scenario, we used a bed area of 20,000 m^2 (= 2 ha), and 20% cover each of algae, *Ruppia* and *Zostera*; these values approximated the mean of each variable (Figures 2.4, 2.6, 2.7 and 2.8). In the first set of scenarios, we simply doubled each SAV variable while keeping the others constant (Table 2.6). Crab density increased most with enhanced algal cover (88.7%), moderately with *Ruppia* (53.3%), and least with *Zostera* (24.4%). For percent cover of all three SAV species, percent changes in crab abundance mirrored those for density. Conversely, crab density decreased 16.0% when bed area was doubled, though crab abundance was raised by 68.1% due to the greater bed area. In the second set of scenarios, we projected alterations in crab density if *Zostera* were to be eradicated from Chesapeake Bay due to climate change (Table 2.6). In one scenario, we eliminated all *Zostera* and kept the other SAV variables constant, which reduced crab density modestly (19.4%). In the other scenarios, we compensated equally for the 20% loss of *Zostera* cover by increasing algal cover and *Ruppia* cover each by 10%. In contrast to the non-compensatory scenario, crab density was raised by 36.7%. Crab abundances were exactly proportional to crab density.

2.5 Discussion

Using temporal distribution patterns of SAV derived from Planet Lab satellite imagery, the main findings were: (i) juvenile blue crab density was inversely related to SAV bed area, but reductions in crab density as bed area increased were more than offset by higher total abundance of crabs as bed area enlarged; (ii) crab density was positively related to percent cover of algae (primarily non-native *Gracilaria vermiculophylla*), widgeon grass *Ruppia maritima* and eelgrass *Zostera marina*; (iii) location, year, season and water depth were not significant predictors of crab density in SAV beds after accounting for the effects of bed area and SAV percent cover; and (iv) potential loss of *Zostera* in Chesapeake Bay due to global warming was projected to cause either only a modest reduction in crab density if other SAV species do not compensate and bed area remains constant, or crab density could

even increase if algae and *Ruppia* were to compensate for the loss of *Zostera*.

Ruppia is better suited than *Zostera* for warmer water temperatures, with *Zostera* ceasing to grow at temperatures above 26.5°C (Richardson et al., 2018). With temperatures above that threshold from June to September in this study, the future of *Zostera* within the York River and lower Chesapeake Bay is uncertain (see Tables 2.3 and 2.4). In the past, *Ruppia* has persisted or even expanded its range when *Zostera* has experienced a die-off (Moore and Jarvis, 2008; Moore et al., 2014; Shields et al., 2019). Hence, *Ruppia* might continue to expand and eventually replace *Zostera* to become the dominant seagrass species.

With the changing conditions expected under climate change, there could be an ecosystem shift within the York River and other tributaries of lower Chesapeake Bay. When conditions drastically change (e.g. warming temperatures), species composition can change, potentially causing a shift to a new equilibrium (May, 1977; Scheffer et al., 2001). Currently, *Zostera* and *Ruppia* are co-dominant seagrass species, with algae (i.e. *Gracilaria* spp.) also present in the system. In the near future, the York River and other lower Chesapeake Bay tributaries may shift to a system dominated by *Ruppia* and algae, with *Zostera* absent or present at much lower abundance. Given future scenarios of climate change, algae and *Ruppia* could compensate for the loss of *Zostera*, acting as an alternative nursery habitat network (Johnston and Lipcius, 2012; Wood, 2017). Algal beds (mostly *Gracilaria* spp.) were a significant predictor of juvenile blue crab density, with algae-only samples having the highest crab densities. This supports the recent suggestion that algal patches serve as an important alternative nursery habitat for juvenile blue crab recruitment in Chesapeake Bay (Johnston and Lipcius, 2012; Wood, 2017).

If the current system in lower Chesapeake Bay with *Zostera* were replaced with one composed of algae and *Ruppia* but not *Zostera*, our simulations indicate that nursery habitat for juvenile blue crabs would remain viable and possibly increase, as long as SAV bed area does not decline sharply. The current climate change scenarios indicate a strong potential

for *Zostera* to be eradicated from Chesapeake Bay (Moore et al., 2014; Richardson et al., 2018; Shields et al., 2019). However, with less inter-specific competition, the distribution of *Gracilaria* and *Ruppia* could expand substantially and compensate for the loss of *Zostera* (Shields et al., 2019).

This study illustrates the value of remote sensing (e.g. satellite imagery) capable of accurately capturing temporal and spatial patterns of habitat distribution. Planet Lab satellite imagery allowed us to quantify the availability of SAV bed habitat during the seasonal blue crab recruitment period, and define how the area of available nursery habitat varies both inter-annually and seasonally within the York River system. Broad-scale data of habitat availability, such as SAV beds, is crucial for addressing the complex issues involving marine resources, like the blue crab, linked to these habitats. Access to accurate satellite imagery will help quantify temporal changes in habitat distribution due to seasonal and episodic disturbances. This information will assist fisheries managers in preparing for future changes in nursery habitat distribution due to climate change and extreme weather events, and thereby effect ecosystem-based fishery management.

Tables

Table 2.1: AIC calculations for the negative binomial regression models corresponding to the different hypotheses for juvenile blue crab density in both 2017 and 2018, denoted by g_i. k = number of parameters, including sample variance (s^2) as a parameter. AIC_c = corrected AIC value. Δ_i = difference between model g_i and the best model. w_i = model probability of fitting the observed data. Abbreviations: Total percent cover = T; Bed area = B; Year = Y; Location = L; algal percent cover = A; *Ruppia maritima* percent cover = R; *Zostera marina* percent cover = Z; Julian day = J; Depth = D.

Model	Variables	k	AIC_c	Δ_i	w_i
g_1	T	3	1383.0	44.9	<0.01
g_2	T + B	4	1374.2	36.1	<0.01
g_3	Y + L + B	5	1414.6	76.4	<0.01
g_4	A + R + Z	5	1340.4	2.3	0.17
g_5	Y + L + T + B	6	1357.7	19.6	<0.01
g_6	**A + R + Z + B**	**6**	**1338.1**	**0**	**0.54**
g_7	Y + L + A + R + Z	7	1341.1	3.0	0.12
g_8	Y + L + A + R + B	7	1351.8	13.7	<0.01
g_9	Y + L + A + Z + B	7	1382.8	44.7	<0.01
g_{10}	Y + L + J + T + B + D	8	1362.0	23.9	<0.01
g_{11}	Y + L + A + R + Z + B	8	1340.8	2.7	0.14
g_{12}	(Y × L) + J + T + B + D	9	1361.3	23.2	<0.01
g_{13}	Y + L + J + A + R + Z + B + D	10	1345.0	6.9	0.02
g_{14}	(Y × L) + J + A + R + Z + B + D	11	1346.9	8.8	<0.01

Table 2.2: Dates of sampling in the York River. A sampling period consisted of one day in 2017 and multiple days in 2018.

2017		2018	
Date	Day of Year	Date	Day of Year
August 10	222	June 19	170
August 15	227	June 25	176
August 31	243	July 2	183
September 14	257	July 3	184
October 5	278	August 6	218
October 19	292	August 8	220
November 16	320	August 20	232
		August 23	235
		August 24	236
		September 4	247
		September 20	263
		October 2	275
		October 3	276
		October 22	295
		October 23	296

Table 2.3: Water quality parameters for 2017 at both Allens Island and the Goodwin Islands. Aug = August; Sept = September; Oct = October; Nov = November.

Location	Date	Temperature (°C)	Salinity	Dissolved Oxygen (mg/L)	Mean Depth (m)
Allens Island	Aug 10	27.8	22.7	10.1	1.1
Goodwin Islands	Aug 10	25.7	22.7	7.8	1.2
Allens Island	Aug 15	28.0	22.4	6.8	1.1
Goodwin Islands	Aug 15	27.4	22.4	6.9	1.0
Allens Island	Aug 31	24.9	21.4	8.4	1.0
Goodwin Islands	Aug 31	24.1	21.4	4.5	0.9
Allens Island	Sept 14	24.3	21.5	9.7	0.9
Goodwin Islands	Sept 14	23.5	22.5	4.5	0.8
Allens Island	Oct 5	23.8	20.7	14.2	0.9
Goodwin Islands	Oct 5	22.9	21.2	8.9	0.8
Allens Island	Oct 19	20.6	22.9	11.7	0.9
Goodwin Islands	Oct 19	19.7	22.4	7.9	0.8
Allens Island	Nov 16	13.4	23.1	11.3	1.0
Goodwin Islands	Nov 16	12.6	22.6	8.7	1.1

Table 2.4: Water quality parameters for 2018 at both Allens Island and the Goodwin Islands. Aug = August; Sept = September; Oct = October; Nov = November.

Location	Date	Mean Temperature (°C)	Mean Salinity	Mean Dissolved Oxygen (mg/L)	Mean Depth (m)
Allens Island	June 19/25	29.1	13.3	6.8	1.0
Goodwin Islands	June 25	28.6	13.3	7.7	0.9
Allens Island	July 2	30.1	12.0	6.6	1.0
Goodwin Islands	July 3	31.2	13.7	6.1	1.0
Allens Island	Aug 6	30.4	14.9	5.9	0.8
Goodwin Islands	Aug 8	30.8	15.3	6.4	0.7
Allens Island	Aug 23	28.6	16.0	5.8	0.5
Goodwin Islands	Aug 20/24	27.2	14.8	5.1	1.1
Goodwin Islands	Sept 4	30.4	14.6	4.8	0.7
Allens Island	Sept 20	26.3	14.4	4.3	1.0
Goodwin Islands	Sept 20	26.6	14.1	4.5	1.0
Allens Island	Oct 3	26.3	13.8	4.9	0.6
Goodwin Islands	Oct 2	25.0	14.3	4.5	0.7
Allens Island	Oct 23	18.0	13.1	5.2	0.6
Goodwin Islands	Oct 22	15.0	11.3	6.2	0.5

Table 2.5: Parameter estimates from negative binomial regression model g_6 for juvenile blue crab density in 2017 and 2018. Percent of deviance explained by the model = 41.6%.

Parameter	Variable	Estimate	SE	p
α	Intercept	2.537	0.150	$<<$0.001
β_1	Algal % cover	0.0317	0.00325	$<<$0.001
β_2	*Ruppia* % cover	0.0213	0.00287	$<<$0.001
β_3	*Zostera* % cover	0.0109	0.00318	$<$0.001
β_4	Bed area	-0.000009	0.000004	0.046

Table 2.6: Simulated crab density under various scenarios of bed area and percent cover of Algae, *Ruppia maritima*, and *Zostera marina* calculated using equation 2.1. ‡Although crab density declined by 16.0%, abundance increased by 35.0% due to the larger bed area.

Conditions	Percent cover Algae	*Ruppia*	*Zostera*	Bed area (m^2)	Crab density (per 1.68 m^2)	% change
Reference	20%	20%	20%	20,000	38.1	
Algae x 2	40%	20%	20%	20,000	71.9	↑ 88.7%
Ruppia x 2	20%	40%	20%	20,000	58.4	↑ 53.3%
Zostera x 2	20%	20%	40%	20,000	47.4	↑ 24.4%
Bed area x 2	20%	20%	20%	40,000	32.0	↓ 16.0%‡
Zostera = 0% (no compensation by Algae or *Ruppia*)						
	20%	20%	0%	20,000	30.7	↓ 19.4%
Zostera = 0% (compensation by Algae + 10% and *Ruppia* + 10%)						
	30%	30%	0%	20,000	52.1	↑ 36.7%

Figures

Figure 2.1: Locations of the two sampling sites within the York River, Allens Island and the Goodwin Islands. The colored portion represents the area used for the remote sensing technique comparison.

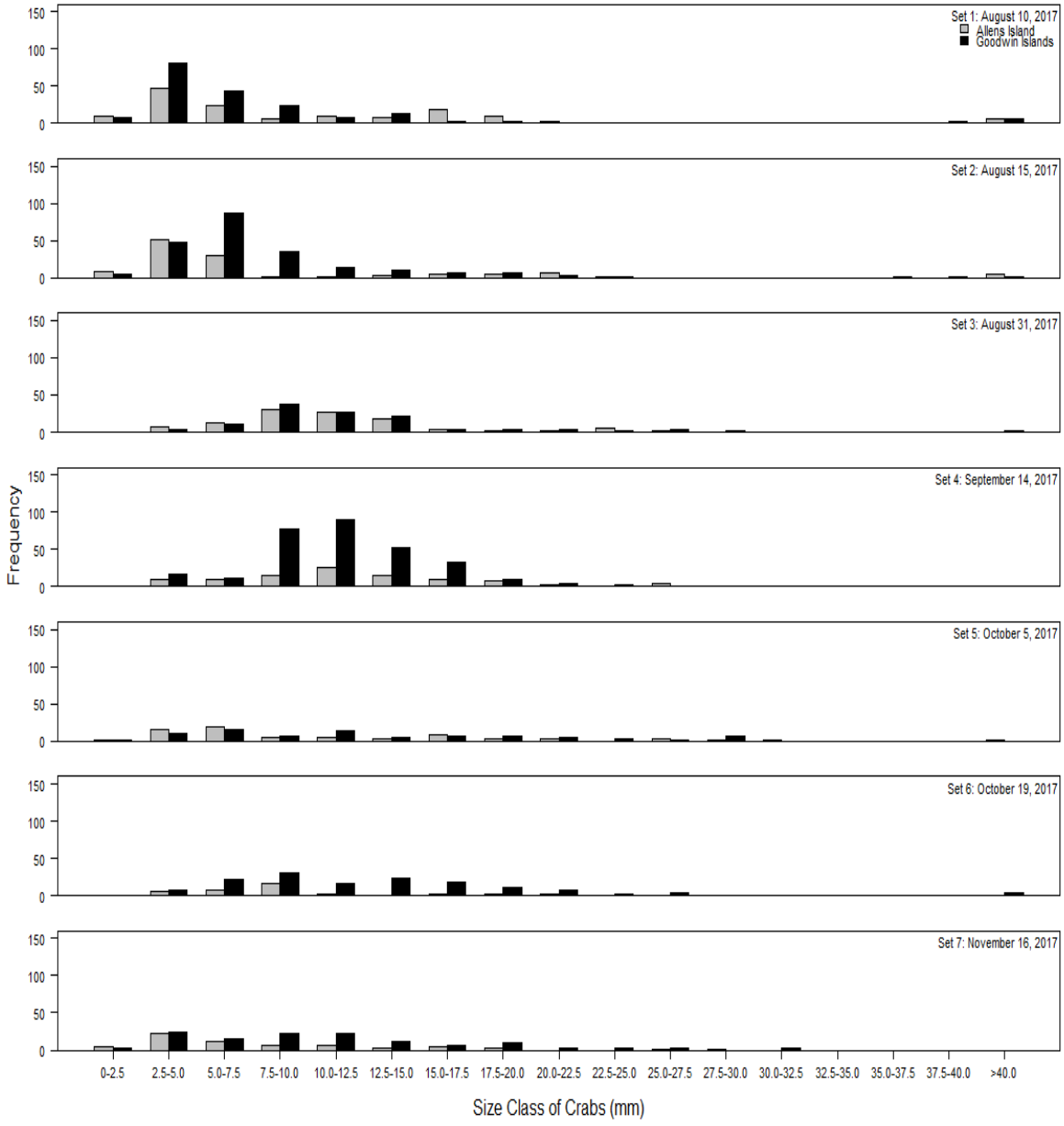

Figure 2.2: Juvenile blue crab data from 2017 grouped into size classes (seven sampling days total). Divisions made every 2.5 mm carapace width, with any crabs above 40 mm grouped in one bin. Allens Island = gray; Goodwin Islands = black.

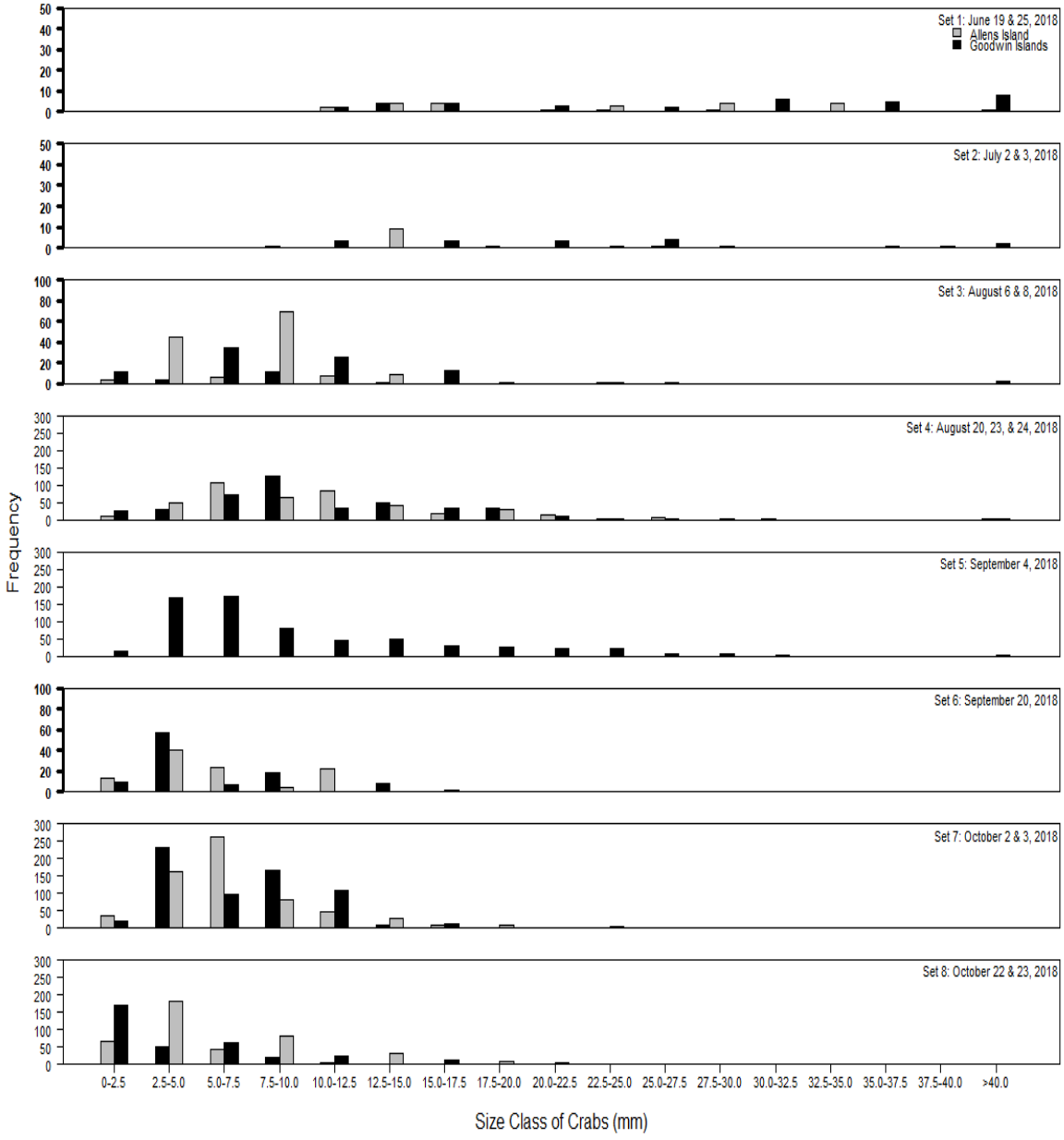

Figure 2.3: Juvenile blue crab data from 2018 grouped into size classes (eight sampling sets; at least one day per site). Divisions made every 2.5 mm carapace width, with any crabs above 40 mm grouped in one bin. Notice the change in axis for sets 1, 2, 3, and 6. Allens Island = gray; Goodwin Islands = black.

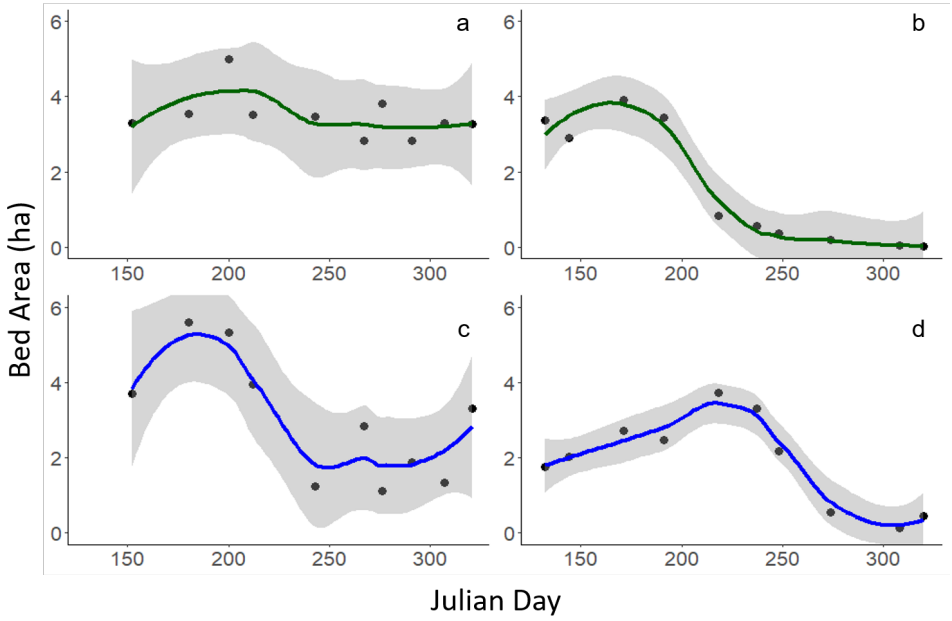

Figure 2.4: Trends in SAV bed area at Allens Island in 2017 (a) and 2018 (b), and the Goodwin Islands in 2017 (c) and 2018 (d). The time series runs from May to November in both years. Calculated using Planet Lab satellite imagery. The curves represent the Loess fit (span = 0.75). The dark grey areas represent the 95% confidence intervals.

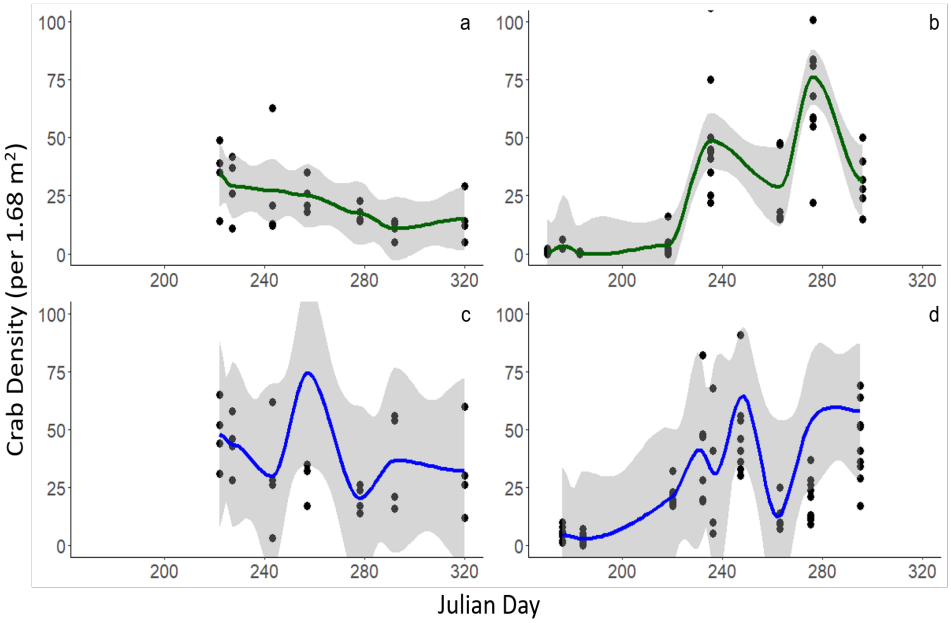

Figure 2.5: Trends in juvenile blue crab density at Allens Island in 2017 (a) and 2018 (b), and the Goodwin Islands in 2017 (c) and 2018 (d). Samples were collected within a 1.68 m^2 drop net; to translate densities to 1 m^2, the graphed values should be multiplied by 0.595. The curves represent the Loess fit (span = 0.25). The dark grey areas represent the 95% confidence intervals.

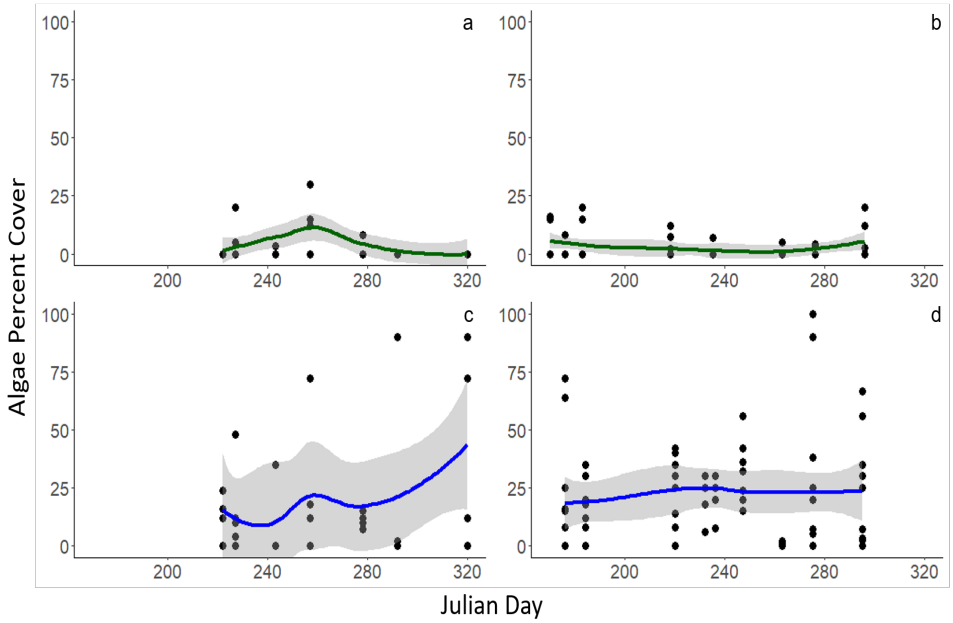

Figure 2.6: Trends in algal percent cover at Allens Island in 2017 (a) and 2018 (b), and the Goodwin Islands in 2017 (c) and 2018 (d). Collected from within 1.68 m^2 drop net. The curves represent the Loess fit (span = 0.75). The dark grey areas represent the 95% confidence intervals.

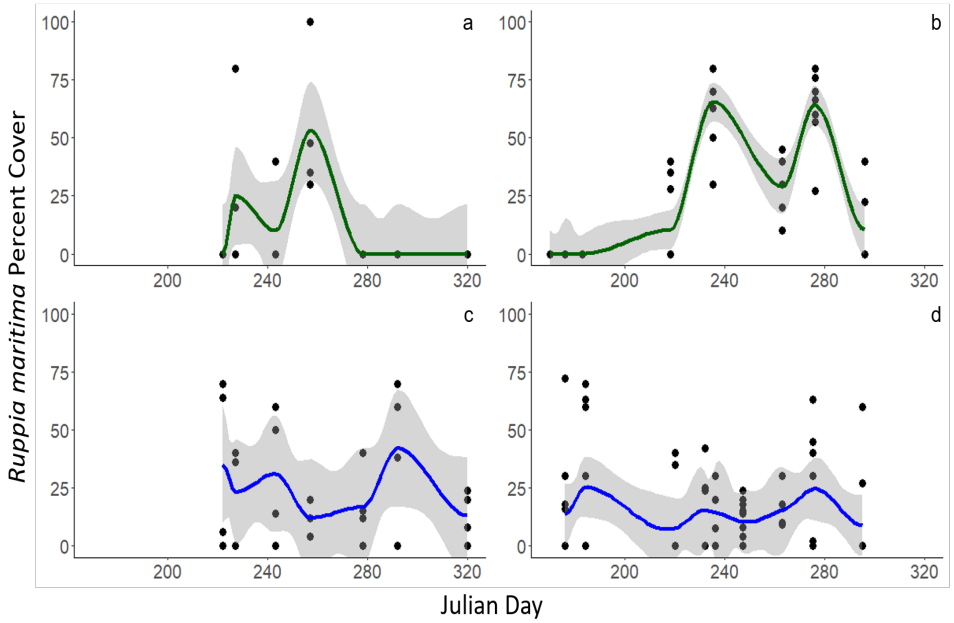

Figure 2.7: Trends in *Ruppia maritima* percent cover at Allens Island in 2017 (a) and 2018 (b), and the Goodwin Islands in 2017 (c) and 2018 (d). Collected from within 1.68 m^2 drop net. The curves represent the Loess fit (span = 0.25). The dark grey areas represent the 95% confidence intervals.

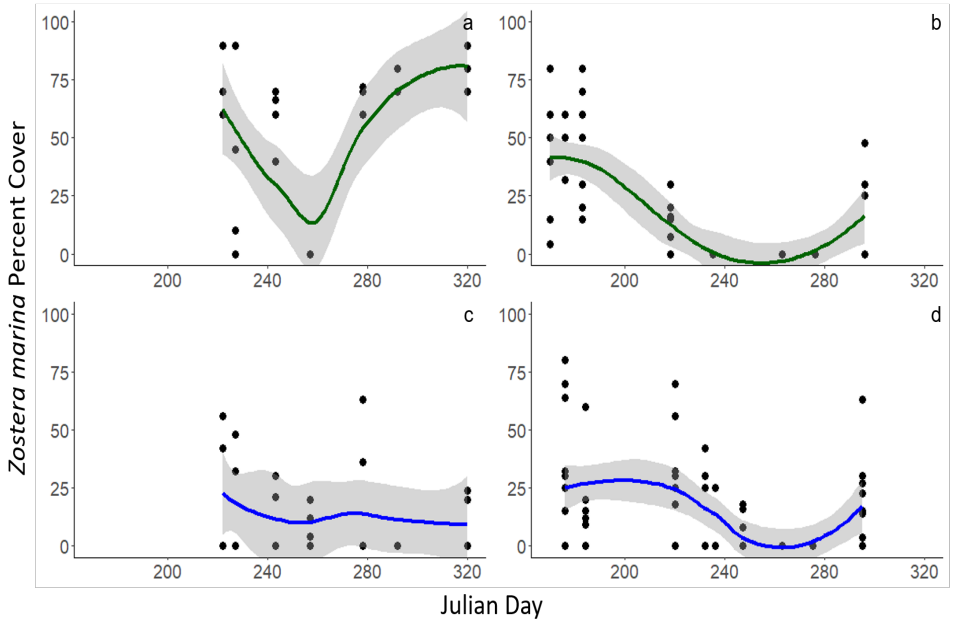

Figure 2.8: Trends in *Zostera marina* percent cover at Allens Island in 2017 (a) and 2018 (b), and the Goodwin Islands in 2017 (c) and 2018 (d). Collected from within 1.68 m^2 drop net. The curves represent the Loess fit (span = 0.75). The dark grey areas represent the 95% confidence intervals.

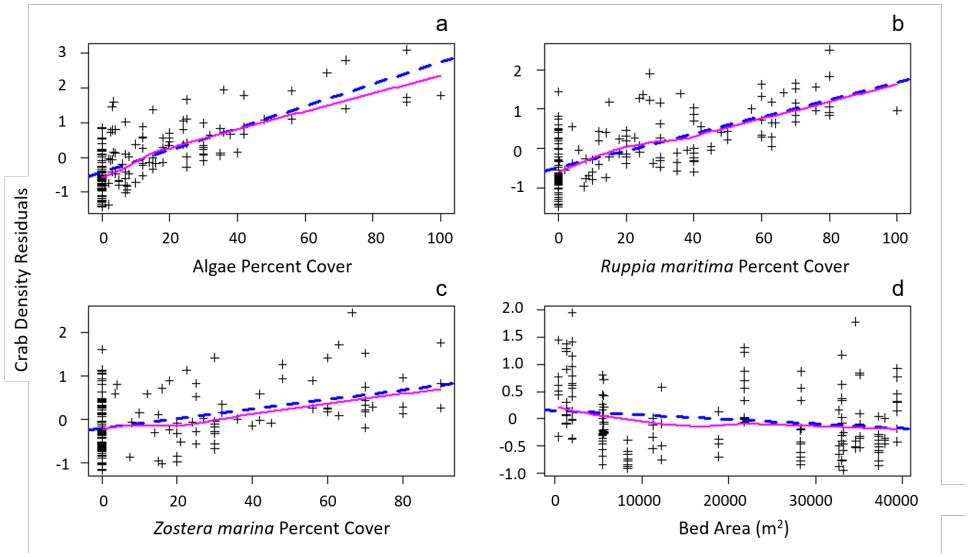

Figure 2.9: Component residual plots for model g_6, which portray the relationship between the dependent variable (juvenile blue crab density) and each independent variable, after accounting for the effects of the other independent variables. The blue dotted line represents the least-squares line. The solid purple line represents the fitted loess line. Algal percent cover (a), *Ruppia maritima* percent cover (b), and *Zostera marina* percent cover (c) all have positive linear relationships with crab density (Table 2.5). Bed area (d) has a negative linear relationship with crab density (Table 2.5).

BIBLIOGRAPHY

Anderson, D.R., 2008. Model based inference in the life sciences: a primer on evidence. Springer Science & Business Media.

Anderson, E.E., 1989. Economic benefits of habitat restoration: Seagrass and the Virginia hard-shell blue crab fishery. North American Journal of Fisheries Management 9, 140–149.

Barbier, E.B., Hacker, S.D., Kennedy, C., Koch, E.W., Stier, A.C., Silliman, B.R., 2011. The value of estuarine and coastal ecosystem services. Ecological Monographs 81, 169–193.

Barillé, L., Robin, M., Harin, N., Bargain, A., Launeau, P., 2010. Increase in seagrass distribution at Bourgneuf Bay (France) detected by spatial remote sensing. Aquatic Botany 92, 185–194.

Beck, M.W., Heck Jr, K.L., Able, K.W., Childers, D.L., Eggleston, D.B., Gillanders, B.M., Halpern, B., Hays, C.G., Hoshino, K., Minello, T.J., et al., 2001. The identification, conservation, and management of estuarine and marine nurseries for fish and invertebrates. Bioscience 51, 633–641.

Boström, C., Jackson, E., Simenstad, C., 2006. Seagrass landscapes and their effects on associated fauna: a review. Estuarine, Coastal and Shelf Science 68, 383–403.

Bromilow, A.M., Lipcius, R.N., 2017. Mechanisms governing ontogenetic habitat shifts: role of trade-offs, predation, and cannibalism for the blue crab. Marine Ecology Progress Series 584, 145–159.

Burnham, K.P., Anderson, D.R., 2002. Model selection and multimodel inference: a practical information-theoretic approach. Springer-Verlag, New York, New York. .

Chamberlin, T.C., 1890. The method of multiple working hypotheses. Science 15, 92–96.

Dekker, A., Brando, V., Anstee, J., Fyfe, S., Malthus, T., Karpouzli, E., 2006. Remote sensing of seagrass ecosystems: use of spaceborne and airborne sensors, in: Larkum, A.W.D., Orth, R.J., Duarte, C. (Eds.), Seagrasses: Biology, Ecology and Conservation. Springer, pp. 347–359.

Dekker, A.G., Brando, V.E., Anstee, J.M., 2005. Retrospective seagrass change detection in a shallow coastal tidal Australian lake. Remote Sensing of Environment 97, 415–433.

ESRI, 2015. ArcGIS Desktop: Release 10.4. Redlands, CA: Environmental Systems Research Institute.

Everett, R.A., Ruiz, G.M., 1993. Coarse woody debris as a refuge from predation in aquatic communities. Oecologia 93, 475–486.

Ferguson, R.L., Korfmacher, K., 1997. Remote sensing and GIS analysis of seagrass meadows in North Carolina, USA. Aquatic Botany 58, 241–258.

Ferwerda, J.G., de Leeuw, J., Atzberger, C., Vekerdy, Z., 2007. Satellite-based monitoring of tropical seagrass vegetation: current techniques and future developments. Hydrobiologia 591, 59–71.

Gullström, M., Lundén, B., Bodin, M., Kangwe, J., Öhman, M.C., Mtolera, M.S., Björk, M., 2006. Assessment of changes in the seagrass-dominated submerged vegetation of tropical Chwaka Bay (Zanzibar) using satellite remote sensing. Estuarine, Coastal and Shelf Science 67, 399–408.

Heck, K.L., Hays, G., Orth, R.J., 2003. Critical evaluation of the nursery role hypothesis for seagrass meadows. Marine Ecology Progress Series 253, 123–136.

Heck, K.L., Thoman, T.A., 1984. The nursery role of seagrass meadows in the upper and lower reaches of the Chesapeake Bay. Estuaries 7, 70–92.

Hines, A.H., 2007. Ecology of juvenile and adult blue crabs, in: Kennedy, V.S., Cronin, L.E. (Eds.), The Blue Crab, Callinectes sapidus. University of Maryland Sea Grant Press. chapter 13, pp. 565–654.

Hines, A.H., Johnson, E.G., Darnell, M.Z., Rittschof, D., Miller, T.J., Bauer, L.J., Rodgers, P., Aguilar, R., 2010. Predicting effects of climate change on blue crabs in Chesapeake Bay. Biology and management of exploited crab populations under climate change. Fairbanks: Alaska Sea Grant, University of Alaska Fairbanks , 109–127.

Hines, A.H., Ruiz, G.M., 1995. Temporal variation in juvenile blue crab mortality: nearshore shallows and cannibalism in Chesapeake Bay. Bulletin of Marine Science 57, 884–901.

Hovel, K.A., Lipcius, R.N., 2001. Habitat fragmentation in a seagrass landscape: patch size and complexity control blue crab survival. Ecology 82, 1814–1829.

Hovel, K.A., Lipcius, R.N., 2002. Effects of seagrass habitat fragmentation on juvenile blue crab survival and abundance. Journal of Experimental Marine Biology and Ecology 271, 75–98.

Howari, F.M., Jordan, B.R., Bouhouche, N., Wyllie-Echeverria, S., 2009. Field and remote-sensing assessment of mangrove forests and seagrass beds in the northwestern part of the United Arab Emirates. Journal of Coastal Research 25, 48–56.

Johnston, C.A., Lipcius, R.N., 2012. Exotic macroalga *Gracilaria vermiculophylla* provides superior nursery habitat for native blue crab in Chesapeake Bay. Marine Ecology Progress Series 467, 137–146.

Koedsin, W., Intararuang, W., Ritchie, R., Huete, A., 2016. An integrated field and remote sensing method for mapping seagrass species, cover, and biomass in southern Thailand. Remote Sensing 8, 292.

Lathrop, R.G., Haag, S.M., Merchant, D., Kennish, M.J., Fertig, B., 2014. Comparison of remotely-sensed surveys vs. in situ plot-based assessments of sea grass condition in Barnegat Bay-Little Egg Harbor, New Jersey, USA. Journal of Coastal Conservation 18, 299–308.

Lefcheck, J.S., Hughes, B.B., Johnson, A.J., Pfirrman, B.W., Rasher, D.B., Smyth, A.R., Williams, B.L., Beck, M.W., Orth, R.J., 2019. Are coastal habitats important nurseries? a meta-analysis. Conservation Letters , e12645.

Lipcius, R.N., Eggleston, D.B., Fodrie, F.J., Van Der Meer, J., Rose, K.A., Vasconcelos, R.P., Van De Wolfshaar, K.E., 2019. Modeling quantitative value of habitats for marine and estuarine populations. Frontiers in Marine Science 6, 280.

Lipcius, R.N., Eggleston, D.B., Heck Jr, K.L., Seitz, R.D., van Montfrans, J., 2007. Ecology of postlarval and young juvenile blue crabs, in: Kennedy, V.S., Cronin, L.E. (Eds.), The Blue Crab, Callinectes sapidus. University of Maryland Sea Grant Press. chapter 13, pp. 535–564.

Lipcius, R.N., Seitz, R.D., Seebo, M.S., Colón-Carrión, D., 2005. Density, abundance and survival of the blue crab in seagrass and unstructured salt marsh nurseries of Chesapeake Bay. Journal of Experimental Marine Biology and Ecology 319, 69–80.

Lyons, M., Phinn, S., Roelfsema, C., 2011. Integrating Quickbird multi-spectral satellite and field data: mapping bathymetry, seagrass cover, seagrass species and change in Moreton Bay, Australia in 2004 and 2007. Remote Sensing 3, 42–64.

Lyons, M.B., Roelfsema, C.M., Phinn, S.R., 2013. Towards understanding temporal and spatial dynamics of seagrass landscapes using time-series remote sensing. Estuarine, Coastal and Shelf Science 120, 42–53.

May, R.M., 1977. Thresholds and breakpoints in ecosystems with a multiplicity of stable states. Nature 269, 471.

Meyer, C.A., Pu, R., 2012. Seagrass resource assessment using remote sensing methods in St. Joseph Sound and Clearwater Harbor, Florida, USA. Environmental Monitoring and Assessment 184, 1131–1143.

van Montfrans, J., Peery, C.A., Orth, R.J., 1990. Daily, monthly and annual settlement patterns by *Callinectes sapidus* and *Neopanope sayi* megalopae on artificial collectors deployed in the York River, Virginia: 1985–1988. Bulletin of Marine Science 46, 214–229.

Moore, K.A., Jarvis, J.C., 2008. Environmental factors affecting recent summertime eelgrass diebacks in the lower chesapeake bay: implications for long-term persistence. Journal of Coastal Research , 135–147.

Moore, K.A., Shields, E.C., Parrish, D.B., 2014. Impacts of varying estuarine temperature and light conditions on *Zostera marina* (eelgrass) and its interactions with *Ruppia maritima* (widgeongrass). Estuaries and Coasts 37, 20–30.

Muller-Karger, F.E., Hestir, E., Ade, C., Turpie, K., Roberts, D.A., Siegel, D., Miller, R.J., Humm, D., Izenberg, N., Keller, M., et al., 2018. Satellite sensor requirements for monitoring essential biodiversity variables of coastal ecosystems. Ecological Applications 28, 749–760.

Mumby, P., Green, E., Edwards, A., Clark, C., 1997. Measurement of seagrass standing crop using satellite and digital airborne remote sensing. Marine Ecology Progress Series 159, 51–60.

Mumby, P., Green, E., Edwards, A., Clark, C., 1999. The cost-effectiveness of remote sensing for tropical coastal resources assessment and management. Journal of Environmental Management 55, 157–166.

National Weather Service, 2019. Wakefield, VA, Forecast Of-

fice. Monthly rainfall analysis. Date accessed: March 12, 2019. <https://www.weather.gov/akq/monthly_rainfall_analysis>.

Orth, R.J., Dennison, W.C., Lefcheck, J.S., Gurbisz, C., Hannam, M., Keisman, J., Landry, J.B., Moore, K.A., Murphy, R.R., Patrick, C.J., et al., 2017a. Submersed aquatic vegetation in Chesapeake Bay: sentinel species in a changing world. Bioscience 67, 698–712.

Orth, R.J., van Montfrans, J., 1987. Utilization of a seagrass meadow and tidal marsh creek by blue crabs *Callinectes sapidus*. I. Seasonal and annual variations in abundance with emphasis on post-settlement juveniles. Marine Ecology Progress Series 41, 283.

Orth, R.J., Moore, K.A., 1986. Seasonal and year-to-year variations in the growth of *Zostera marina* l. (eelgrass) in the lower Chesapeake Bay. Aquatic Botany 24, 335–341.

Orth, R.J., Wilcox, D.J., Whiting, J.R., Kenne, A.K., Smith, E.R., 2018. 2017 Distribution of Submerged Aquatic Vegetation in the Chesapeake Bay and Coastal Bays. Final report to EPA, Chesapeake Bay Program, Annapolis, MD. Grant No CB96343701-0. <http://www.vims.edu/bio/sav/sav17>.

Orth, R.J., Wilcox, D.J., Whiting, J.R., Kenne, A.K., Smith, E.R., Nagey, L., 2017b. 2016 Distribution of Submerged Aquatic Vegetation in the Chesapeake Bay and Coastal Bays. VIMS Special Scientific Report Number 160. Final report to EPA, Chesapeake Bay Program, Annapolis, MD. Grant No CB96343701-0. <http://www.vims.edu/bio/sav/sav16>.

Pardieck, R.A., Orth, R.J., Diaz, R.J., Lipcius, R.N., 1999. Ontogenetic changes in habitat use by postlarvae and young juveniles of the blue crab. Marine Ecology Progress Series 186, 227–238.

Perkins-Visser, E., Wolcott, T.G., Wolcott, D.L., 1996. Nursery role of seagrass beds:

enhanced growth of juvenile blue crabs (callinectes sapidus rathbun). Journal of Experimental Marine Biology and Ecology 198, 155–173.

Pile, A.J., Lipcius, R.N., van Montfrans, J., Orth, R.J., 1996. Density-dependent settler-recruit-juvenile relationships in blue crabs. Ecological Monographs 66, 277–300.

Planet Team, 2019. Planet Application Program Interface: In space for life on Earth. <https://api.planet.com>.

Pu, R., Bell, S., Levy, K.H., Meyer, C., 2010. Mapping detailed seagrass habitats using satellite imagery, in: 2010 IEEE International Geoscience and Remote Sensing Symposium, IEEE. pp. 1–4.

Ralph, G.M., Seitz, R.D., Orth, R.J., Knick, K.E., Lipcius, R.N., 2013. Broad-scale association between seagrass cover and juvenile blue crab density in Chesapeake Bay. Marine Ecology Progress Series 488, 51–63.

Richardson, J.P., Lefcheck, J.S., Orth, R.J., 2018. Warming temperatures alter the relative abundance and distribution of two co-occurring foundational seagrasses in Chesapeake Bay, USA. Marine Ecology Progress Series 599, 65–74.

Roelfsema, C., Kovacs, E.M., Saunders, M.I., Phinn, S., Lyons, M., Maxwell, P., 2013. Challenges of remote sensing for quantifying changes in large complex seagrass environments. Estuarine, Coastal and Shelf Science 133, 161–171.

Roelfsema, C., Phinn, S., Udy, N., Maxwell, P., 2009. An integrated field and remote sensing approach for mapping seagrass cover, Moreton Bay, Australia. Journal of Spatial Science 54, 45–62.

RStudio Team, 2016. RStudio: Integrated development for R. RStudio, Inc. <http://www.rstudio.com>.

Scheffer, M., Carpenter, S., Foley, J.A., Folke, C., Walker, B., 2001. Catastrophic shifts in ecosystems. Nature 413, 591.

Seitz, R.D., Lipcius, R.N., Knick, K.E., Seebo, M.S., Long, W.C., Brylawski, B.J., Smith, A., 2008. Stock enhancement and carrying capacity of blue crab nursery habitats in Chesapeake Bay. Reviews in Fisheries Science 16, 329–337.

Seitz, R.D., Lipcius, R.N., Seebo, M.S., 2005. Food availability and growth of the blue crab in seagrass and unvegetated nurseries of Chesapeake Bay. Journal of Experimental Marine Biology and Ecology 319, 57–68.

Seitz, R.D., Wennhage, H., Bergström, U., Lipcius, R.N., Ysebaert, T., 2014. Ecological value of coastal habitats for commercially and ecologically important species. ICES Journal of Marine Science 71, 648–665.

Sharov, A., Vølstad, J., Davis, G., Davis, B., Lipcius, R., Montane, M., 2003. Abundance and exploitation rate of the blue crab (*Callinectes sapidus*) in Chesapeake Bay. Bulletin of Marine Science 72, 543–565.

Shields, E.C., Parrish, D., Moore, K., 2019. Short-term temperature stress results in seagrass community shift in a temperate estuary. Estuaries and Coasts 42, 755–764.

Stockhausen, W.T., Lipcius, R.N., 2003. Simulated effects of seagrass loss and restoration on settlement and recruitment of blue crab postlarvae and juveniles in the York River, Chesapeake Bay. Bulletin of Marine Science 72, 409–422.

Thomsen, M.S., Staehr, P.A., Nyberg, C.D., Schwærter, S., Krause-Jensen, D., Silliman, B.R., 2007. *Gracilaria vermiculophylla* (Ohmi) Papenfuss, 1967 (Rhodophyta, Gracilariaceae) in northern Europe, with emphasis on Danish conditions, and what to expect in the future. Aquatic Invasions 2, 83–94.

Vasconcelos, R.P., Eggleston, D.B., Le Pape, O., Tulp, I., 2014. Patterns and processes of habitat-specific demographic variability in exploited marine species. ICES Journal of Marine Science 71, 638–647.

Venables, W., Ripley, B., Isbn, S., 2002. Statistics complements to modern applied statistics with s fourth edition by .

Virginia Institute of Marine Science, 2018. Winter Dredge Survey. <http://www.vims.edu/research/units/programs/bc_winter_dredge/index.php>.

Vuong, Q.H., 1989. Likelihood ratio tests for model selection and non-nested hypotheses. Econometrica: Journal of the Econometric Society , 307–333.

Wilson, K.A., Able, K.W., Heck Jr, K.L., 1990. Predation rates on juvenile blue crabs in estuarine nursery habitats: evidence for the importance of macroalgae (*Ulva lactuca*). Marine Ecology Progress Series 58, 243–251.

Wood, M.A., 2017. Juvenile Blue Crab (*Callinectes sapidus*) Response to Altered Nursery Habitat. Ph.D. thesis. The College of William and Mary.

Yang, D., Yang, C., 2009. Detection of seagrass distribution changes from 1991 to 2006 in Xincun Bay, Hainan, with satellite remote sensing. Sensors 9, 830–844.